The Reactor Antineutrino Anomaly

G. Mention,[1] M. Fechner,[1] Th. Lasserre,[1,2,*] Th. A. Mueller,[3] D. Lhuillier,[3] M. Cribier,[1,2] and A. Letourneau[3]

[1] *CEA, Irfu, SPP, Centre de Saclay, F-91191 Gif-sur-Yvette, France*
[2] *Astroparticule et Cosmologie APC, 10 rue Alice Domon et Leonie Duquet, 75205 Paris cedex 13, France*
[3] *CEA, Irfu, SPhN, Centre de Saclay, F-91191 Gif-sur-Yvette, France*

(Dated: January 14, 2011)

Recently, new reactor antineutrino spectra have been provided for ^{235}U, ^{239}Pu, ^{241}Pu, and ^{238}U, increasing the mean flux by about 3 percent. To a good approximation, this reevaluation applies to all reactor neutrino experiments. The synthesis of published experiments at reactor-detector distances <100 m leads to a ratio of observed event rate to predicted rate of 0.979±0.029. With our new flux evaluation, this ratio shifts to 0.937±0.027, leading to a deviation from unity at 98.4% C.L. which we call the reactor antineutrino anomaly. The compatibility of our results with the existence of a fourth non-standard neutrino state driving neutrino oscillations at short distances is discussed. The combined analysis of reactor data, gallium solar neutrino calibration experiments, and MiniBooNE-ν data disfavors the no-oscillation hypothesis at 99.93% C.L. The oscillation parameters are such that $|\Delta m^2_{new}| > 1.5$ eV^2 (99%) and $\sin^2(2\theta_{new}) = 0.17 \pm 0.1$ (95%). Constraints on the θ_{13} neutrino mixing angle are revised.

I. INTRODUCTION

Neutrino oscillation experiments over the last twenty years have established a picture of neutrino mixing and masses that explains the results of solar, atmospheric and reactor neutrino experiments [1]. These experiments are consistent with the mixing of ν_e, ν_μ and ν_τ with three mass eigenstates, ν_1, ν_2 and ν_3. In particular, the mass differences are required to be $|\Delta m^2_{31}| \cong 2.4\,10^{-3}$eV^2 and $\Delta m^2_{21}/\Delta m^2_{31} \cong 0.032$.

Reactor experiments have played an important role in the establishment of this pattern. In experiments at distances <100 m from the reactor core, at ILL-Grenoble, Goesgen, ROVNO, Krasnoyarsk, and Bugey [2–8], the measured rate of $\bar{\nu}_e$ was found in reasonable agreement with that predicted from the reactor antineutrino spectra, though slightly lower than expected, with the measured/expected ratio at 0.979±0.029 (including recent revisions of the neutron mean lifetime). This opened the way to longer baseline experiments measuring the $\bar{\nu}_e$ survival probability P_{ee} at various distances.

Including the three known active neutrinos P_{ee} can be written in first approximation as,

$$P^{2\nu}_{ee}(L) = 1 - \sin^2(2\theta_i)\cdot\sin^2\left(1.27\frac{\Delta m^2_i[\mathrm{eV}^2]L[\mathrm{m}]}{E_{\bar{\nu}_e}[\mathrm{MeV}]}\right), \quad (1)$$

where $\Delta m^2_i = \Delta m^2_{21}$ and $\theta_i \sim \theta_{12}$ if the baseline exceeds a few tens of kilometers, and $\Delta m^2_i = \Delta m^2_{31}$ and $\theta_i = \theta_{13}$ if it does not exceed a few kilometers [9].

The CHOOZ experiment was located 1 km away from two 4.3 GW reactors [10], and did not report any neutrino oscillation in the parameter region $\Delta m^2_{31} > 10^{-3}$eV^2. In addition CHOOZ data provides the world's best constraint on the θ_{13} mixing angle value, at $\sin^2(2\theta_{13}) < 0.14$ (90% C.L.) for $|\Delta m^2_{31}| \cong 2.40\,10^{-3}$eV^2. Forthcoming kilometer baseline experiments with multiple detectors are underway to provide a clean measurement of the last undetermined neutrino mixing angle θ_{13} [11–13].

The KamLAND experiment detected electron antineutrinos from surrounding reactors located at an average distance of 180 km, thus probing the $\Delta m^2_{21} \sim 10^{-4}$ eV^2 region. KamLAND successfully reported a strong oscillation signal in agreement with solar neutrino data [14]. A three-flavor oscillation treatment shows that KamLAND also has a weak sensitivity to the θ_{13} mixing angle, as $P_{ee} \sim \cos^4(\theta_{13})P^{2\nu}_{ee}$, leading to the anti-correlation of $\sin^2\theta_{13}$ and $\sin^2(\theta_{12})$. Recent global fits including solar neutrino and reactor oscillation data indicated a preference for non-zero θ_{13} at about 1.5σ [15].

In preparation for the Double Chooz reactor experiment, we have re-evaluated the specific reactor antineutrino flux (ν/fission), improving the electron to antineutrino data conversion [16]. The method relies on detailed knowledge of the decays of thousands of fission products, while the previous conversion procedure used a phenomenological model based on 30 effective beta branches. Both methods are constrained by the well-measured ILL spectrum of fission induced electrons that accompanies the antineutrinos [17–20].

The new calculation results in a small increase in the flux of 3.5%. Although this increase has no significant effect on KamLAND's solar parameter results, when combined with the previously reported small deficits at nearer distances, it results in a larger average deficit of 6.2%, at 0.937±0.027. We call it the reactor antineutrino anomaly, significant at the level of 2.14σ (98.4% C.L.). This deficit is consistent with being independent from the distance to the reactor core at distances $\gtrsim 15$ meters, the distance of the Bugey-3 experiment [4].

If this deficit is due to neutrino mixing, it could be explained by an energy-independent suppression of the $\bar{\nu}_e$ flux at distances $\gtrsim 15$ meters. This requires a neutrino with a $|\Delta m^2_{new}| \gtrsim 1$ eV^2. The mixing amplitude with the

* Corresponding author: thierry.lasserre@cea.fr

ν_e must be $\sin^2(2\theta_{new}) \sim 0.17$. The required $|\Delta m^2_{new}|$ is significantly larger than those required by solar and atmospheric experiments. This suggests, if the neutrino mixing hypothesis is the correct explanation, the existence of a fourth neutrino, beyond the standard model. We would like to stress here that other explanations are also possible, such as a correlated artifact in the experiments, or an erroneous prediction of the antineutrino flux from the nuclear reactor cores.

We begin by discussing the use of new antineutrino spectra and provide a revised value of the predicted cross section per fission, in Section II. We then revisit the short baseline oscillation results (<100 m) and CHOOZ in Section III, revealing a reactor antineutrino anomaly, which is discussed in Section IV. The compatibility of our results with the existence of a fourth non-standard neutrino state is discussed in Section V. The CHOOZ and KamLAND sensitivities to the θ_{13} mixing angle are revisited in Sections VI A and VI B. Their combination is discussed in Section VI C. Two experimental programs for testing the anomaly are discussed in Section VII. We conclude in Section VIII.

II. NEW PREDICTED CROSS SECTION PER FISSION

Fission reactors release about 10^{20} $\bar{\nu}_e$ GW^{-1}s^{-1}, which mainly come from the beta decays of the fission products of ^{235}U, ^{238}U, ^{239}Pu, and ^{241}Pu. The emitted antineutrino spectrum is then given by:

$$S_{tot}(E_\nu) = \sum_k f_k S_k(E_\nu), \quad (2)$$

where f_k refers to the contribution of the main fissile nuclei to the total number of fissions of the kth branch, and S_k to their corresponding neutrino spectrum.

For the last 25 years the $\bar{\nu}_e$ spectra have been estimated from measurements of the total electron spectra associated with the beta decays of all fission products of ^{235}U, ^{239}Pu, and ^{241}Pu. Thin target foils of these isotopes were irradiated with thermal neutrons at the ILL reactor [18–20]. The measured spectra then had to be converted from electron to antineutrino spectra invoking a set of 30 effective beta-branches, adjusted to reproduce the total electron spectrum [26].

Recently we revisited the conversion procedure with a novel mixed-approach combining the accurate reference of the ILL electron spectra with the physical distribution of beta branches of all fission products provided by the nuclear databases [16]. This new approach provided a better handle on the systematic errors of the conversion. Although it did not reduce the final error budget, it led to a systematic shift of about 3% in the normalization of ^{235}U, ^{239}Pu, and ^{241}Pu antineutrino fluxes, respectively. This normalization shift has been attributed to two main systematic effects in the original conversion of the ILL electron data. At low energy (E_ν <4 MeV) the implementation of Coulomb and weak magnetism corrections to the Fermi theory in the new approach turned out to deviate from the effective linear correction ($0.65\times(E_\nu - 4$ MeV) in %) used in the previous work. At high energy (E_ν >4 MeV), the converted antineutrino spectra become very sensitive to the knowledge of the charge Z of the nuclei contributing to the total spectrum. In the previous approach, only the mean dependence of Z versus the end-point of the effective beta-branches had been used while in the new conversion we had access to the complete distribution, nucleus by nucleus. These two effects could be numerically studied and confirmed on various independent sets of beta-branches.

Because ^{238}U nuclei undergo fission with fast neutrons, the associated electron spectrum could not be measured in the thermal neutron flux of the ILL reactor. Therefore the *ab initio* summation of the $\bar{\nu}_e$ from all possible beta decays of fission products was performed to predict the neutrino spectrum [21]. In Ref. [16] we provided a new prediction with an estimated relative uncertainty of the order of 15% in the 2-8 MeV range. This uncertainty of *ab initio* calculations is still too large to be generalized to all isotopes but it is sufficiently accurate in the case of ^{238}U, which contributes to less than 10% of the total fission rate for all reactors considered in this work. An ongoing measurement at the FRM II reactor in Garching will soon provide experimental constraints [22].

When predicting the antineutrino spectrum of a reactor $S_{tot}(E_\nu)$, a weighted sum of the four antineutrino spectra $S_k(E_\nu)$ is computed according to the considered fuel composition, different in each experiment. The object of this article is to analyze the impact of the abovementioned ∼3 percent shifts on past, present, and future experiments.

Generally reactor neutrino oscillation experiments search for the reaction:

$$\bar{\nu}_e + p \rightarrow e^+ + n, \quad (3)$$

where an electron antineutrino interacts with a free proton in a detector, often filled with scintillator. The reaction cross section can be precisely computed with the V-A theory of weak interaction:

$$\sigma_{\mathrm{V-A}}(E_e) = \frac{2\pi\hbar^3}{m_e^5 c^7 f \tau_n} p_e E_e (1 + \delta_{rec} + \delta_{wm} + \delta_{rad}), \quad (4)$$

τ_n being the neutron mean lifetime, p_e and E_e the momentum and energy of the positron, and the δ being the energy dependent recoil (δ_{rec}), weak magnetism (δ_{wm}), and radiative (δ_{rad}) corrections. f is the usual statistical function including the Coulomb correction for Z=1 [26]. The outgoing positron and incoming antineutrino energies are related by $E_\nu = E_e + (M_n - M_p)c^2$.

The prediction of the cross section per fission is defined as:

$$\sigma_f^{pred} = \int_0^\infty S_{tot}(E_\nu)\sigma_{\mathrm{V-A}}(E_\nu)dE_\nu = \sum_k f_k \sigma_{f,k}^{pred}, \quad (5)$$

where S_{tot} is the model dependent reactor neutrino spectrum for a given average fuel composition and $\sigma_{\mathrm{V-A}}$ is the theoretical cross section of reaction (3). The $\sigma_{f,k}^{pred}$ are the predicted cross sections for each fissile isotope. Experiments at baselines $<$ 100 m reported either the ratios of the measured to predicted cross section per fission, or the ratios (R) of the observed event rate to the predicted rate.

Over the last 15 years the neutron mean lifetime evolved, from 926 s (value used in the ILL experiment [2]) to its PDG average value [1]. We corrected its value separately for each experiment. In Bugey-4 for instance its leads to a +0.2% increase of $\sigma_{\mathrm{V-A}}$.

Accounting for new reactor antineutrino spectra [16] the normalization of predicted antineutrino rates, $\sigma_{f,k}^{pred}$, shifts by +2.5%, +3.1%, +3.7%, +9.8% for k=^{235}U, ^{239}Pu, ^{241}Pu, and ^{238}U respectively (see Table I). In the case of ^{238}U the completeness of nuclear databases over the years largely explains the +9.8% shift from the reference computations [21]. The new predicted cross section for any fuel composition can be computed from Eq. (5). By default our new computation takes into account the so-called off-equilibrium correction of the antineutrino fluxes (increase in fluxes caused by the decay of long-lived fission products).

III. IMPACT ON PAST EXPERIMENTAL RESULTS

In the eighties and nineties, experiments were performed at a few tens of meters from nuclear reactor cores at ILL, Goesgen, ROVNO, Krasnoyarsk, and Bugey (so called -3 and -4) [2–8]. Following these pioneering results middle- and long-baseline experiments were performed at CHOOZ [10] and KamLAND [14] in the late nineties and after. In this section we revised each ratio of observed event rate to predicted rate. The observed event rates and their associated errors are unchanged. The predicted rates are reevaluated separately in each experimental case.

A. The Bugey-4 integral measurement

The Bugey-4 experiment [3] performed the most precise measurement of the neutron inverse beta decay cross section, obtaining σ_f^{bugey}=5.752±0.081 in units of 10^{-43} cm^2/fission. This experimental result was compared to the predicted cross section per fission, $\sigma_f^{pred,old}$.

Using Ref. [3] inputs, and the former converted neutrino spectra from [18, 27, 28] (except for the ^{238}U neutrino spectrum taken from [16]), we get $\sigma_f^{pred,old}$=5.850 10^{-43} cm^2/fission, in good agreement with Bugey-4's estimation (see Table I). We used the average fuel composition of Ref. [3], ^{235}U=53.8%, ^{239}Pu=32.8%, Pu^{241}=5.6% and U^{238}=7.8%, in fractions of fissions per isotope. We note here that the published Bugey-4 cross section calculation does not account for the contribution of long-lived fission products (off-equilibrium effects). The reference electron spectra used for the determination of S_{tot} were acquired after an irradiation time in the ILL reactor flux of less than 1.5 day for all isotopes. But in Bugey experiments at a commercial PWR the irradiation time scale was typically of the order of the year. S_{tot} should thus be corrected for the accumulation of long lifetime fission products in the low energy part of the spectrum. We had to switch them off in our computation to recover the $\sigma_f^{pred,old}$ value. Including these effects in our calculations would lead to a +1.0% discrepancy. An over- or underestimation of the irradiation time by 100 days would lead to a systematic error on the off-equilibrium correction below 0.1%.

	old [3]	new
$\sigma_{f,^{235}U}^{pred}$	6.39±1.9%	6.61±2.11%
$\sigma_{f,^{239}Pu}^{pred}$	4.19±2.4%	4.34±2.45%
$\sigma_{f,^{238}U}^{pred}$	9.21±10%	10.10±8.15%
$\sigma_{f,^{241}Pu}^{pred}$	5.73±2.1%	5.97±2.15%
σ_f^{pred}	5.824±2.7%	6.102±2.7%
σ_f^{bugey}	5.752±1.4% [3]	
$\sigma_f^{bugey}/\sigma_f^{pred}$	0.987±1.4%±2.7%	0.943±1.4%±2.7%

TABLE I. Individual cross sections per fission per fissile isotope, $\sigma_{f,k}^{pred}$. The slight differences in the ratios are caused by differences in off-equilibrium effects. Results of the comparison of σ_f^{bugey} at Bugey-4 in units of 10^{-43} cm^2/fission with the former and present prediction, σ_f^{pred}, are shown.

Computing the ratio of observed versus expected events R_{bugey}=$\sigma_f^{bugey}/\sigma_f^{pred}$, Bugey-4 concluded that there was good agreement with the V-A theory of weak interactions, and that the neutrino flux emitted by PWR reactors is sufficiently understood to be computed using the parameters of [18, 27, 28].

Applying the new reactor antineutrino spectra we obtain a new value of the cross section per fission of $\sigma_f^{pred,new}$=6.102±0.163 10^{-43} cm^2/fission. We thus revised the ratio $R_{bugey-4}$=0.943 ± 0.013($stat$) ± 0.025($syst$), which is now 2.0 standard deviations from the expectation without neutrino oscillations. This creates a tension between the measurement at Bugey-4 and the new predicted cross section per fission. In the next sections we will see that the other reactor neutrino experimental results confirm this anomaly.

B. The ILL neutrino experiment

In the early eighties the ILL experiment measured the antineutrino induced positron spectrum at a distance of 8.76 m from the core of the Laue-Langevin fission reactor.

Its fuel is highly enriched uranium in ^{235}U, at 93%, simplifying the computation of the predicted antineutrino spectrum rate and shape. In Ref. [2] the ILL experiment reported a ratio of measured to predicted event rates of $R_{ILL,80}$=0.955 ± 0.035($stat$) ± 0.11($syst$).

In 1995 this result was revised by part of the ILL collaboration [23]. The 1980 reactor electron spectrum for ^{235}U of Ref. [17] was re-measured in 1984 [18] by the same authors as [17]. The neutron mean lifetime was corrected from 926 s to 889 s, increasing the predicted cross section by 4%. Moreover in 1990 it was announced that the operating power of the ILL reactor had been incorrectly reported at the time of the neutrino experiment, by +9.5%. This reanalysis led to $R_{ILL,95}$=0.832±0.029($stat$)±0.0738($syst$), excluding the no-oscillation case at 2 σ.

According to the new spectra of Ref. [16] the antineutrino rate is increased by ∼3.5% (see Table II). A slight neutron mean lifetime correction leads to an additional +0.37% shift. The new ratio is thus $R_{ILL,new}$=0.800 ± 0.028($stat$) ± 0.071($syst$), significantly deviating from its expected value.

	old	new	err(%)	corr(%)	L(m)
Bugey-4	0.987	0.943	3.0	3.0	14
ROVNO	0.985	0.940	3.9	3.0	18
Bugey-3	0.988	0.943	5.0	5.0	14
Bugey-3	0.994	0.948	5.1	5.0	40
Bugey-3	0.915	0.873	14.1	5.0	95
Goesgen	1.018	0.971	6.5	6.0	38
Goesgen	1.045	0.997	5.4	6.0	45
Goesgen	0.975	0.930	7.6	6.0	65
ILL	0.832	0.800	7.4	6.0	9
Krasn. I	1.013	0.944	5.1	4.1	33
Krasn. II	1.031	0.954	20.3	4.1	92
Krasn. II	0.989	0.954	4.1	4.1	57
PaloVerde	1.011	0.975	6.1	—	820
CHOOZ	1.01	0.961	4.3	—	1050

TABLE II. N_{obs}/N_{pred} ratios based on old and new spectra. Off-equilibrium corrections have been applied when justified. The err column is the total error published by the collaborations including the error on S_{tot}, the corr column is the part of the error correlated among multiple-baseline experiments, or experiments using the same detector. This table is used to construct to covariance matrix (Eq. 7).

C. Bugey-3, Goesgen, Krasnoyarsk, ROVNO

We now study the impact of the new antineutrino spectra on experiments at Bugey (called Bugey-3), Goesgen, ROVNO, and Krasnoyarsk [4–7], which measured the reactor antineutrino rate at short distances, between 14 m and 95 m, but less accurately than Bugey-4 [3].

Accounting for new reactor antineutrino spectra [16] the Bugey-3 [4] ratios of observed versus expected events between 1 and 6 MeV decrease by 3.7%. However, we have to apply a further correction to account for the off-equilibrium effects. Assuming 300 days of irradiation this leads to an additional increase by +1.0%. The Bugey-3 ratios become: 0.943 ± 0.037($stat$) ± 0.044($syst$) at 15 m, 0.948 ± 0.01($stat$) ± 0.045($syst$) at 40 m and 0.873 ± 0.10($stat$) ± 0.041($syst$) at 95 m. Note that uncertainties on S_{tot} are included in the errors quoted by the Bugey-3 collaboration.

A similar analysis is performed with the Goesgen [5] results. The new Goesgen ratios shift to 0.971 ± 0.017($stat$) ± 0.015($syst$) at 38 m, 0.997 ± 0.019($stat$) ± 0.015($syst$) at 45 m and 0.930 ± 0.033($stat$) ± 0.028($syst$) at 65 m. We quote here the corrected ratios, not including the uncertainties on S_{tot} to allow for a simple comparison with Ref. [5].

In 1983 the ROVNO integral experiment [6] measured a cross section per fission of σ_f^{ROVNO} = 5.85 ± 0.17 in units of 10^{-43} cm^2/fission, 18 m away from a nuclear core with an average fuel composition of ^{235}U=61.4%, ^{239}Pu=27.5%, Pu^{241}=3.1% and U^{238}=7.4%. They predicted the cross section $\sigma_{f,ROVNO}^{pred,old}$ = 5.94 ± 0.16 in units of 10^{-43} cm^2/fission, and thus obtained the ratio $R_{ROVNO,old}$=0.985 ± 0.037($stat+syst$). We recomputed the cross section per fission according to the new antineutrino spectra and found $\sigma_{f,ROVNO}^{pred,new}$ = 6.223 ± 0.17. The new ratio is thus revised to $R_{ROVNO,new}$=0.940 ± 0.036($stat+syst$). We note that the correction of the neutron mean lifetime contributes 1.8% to the shift of the ratio.

In 1984 a neutrino experiment operated at the Krasnoyarsk reactors [7], which have an almost pure ^{235}U fuel composition leading to an antineutrino spectrum within 1% of pure ^{235}U, and operate over 50 day cycles. They measured the cross section per fission at two distances, $\sigma_f^{Krasno,33m}$ = 6.19 ± 0.36 at 33 m and $\sigma_f^{Krasno,92m}$ = 6.30 ± 1.28 at 92 m, in units of 10^{-43} cm^2/fission. They compared it to the predicted cross section of 6.11 ± 0.21 10^{-43} cm^2/fission, based on the Ref. [17] ^{235}U measurement instead of Ref. [18]. Correcting the neutron mean lifetime and using the new antineutrino spectra we obtain a predicted cross section of 6.56 10^{-43} cm^2/fission, assuming a pure ^{235}U spectrum. This leads to the ratios $R_{Krasno,33m}$=0.944±0.048($stat+syst$) and $R_{Krasno,92m}$=0.954 ± 0.219($stat+syst$), at 33 m and 92 m, respectively. In 1994 two other measurements were performed 50.0 m and 50.7 m from the Krasnoyarsk reactors [8]. They measured $\sigma_f^{Krasno,50m}$ = 6.26 ± 0.26 at 50 m, and compared it to their predicted cross section of 6.33 ± 0.19 10^{-43} cm^2/fission, based on Ref. [18] and in agreement with our reevaluation using previous reference antineutrino spectra. Using the new values of Ref. [16] we revise the ratio $R_{Krasno,50m}$=0.954 ± 0.040($stat+syst$).

D. CHOOZ and Palo Verde

Based on the good agreement between $\sigma_f^{pred,old}$ and σ_f^{bugey} obtained in Bugey-4 [3], the CHOOZ experiment [10] decided to use the total cross section per fission measured in the Bugey-4 measurement, correcting a posteriori for the different averaged fuel composition according to:

$$\sigma_f^{chooz} = \sigma_f^{bugey} + \sum_k (f_k^{chooz} - f_k^{bugey})\sigma_{f,k}^{pred,old}, \quad (6)$$

where f_k^{chooz} and f_k^{bugey} are the contributions of the k^{th} isotope to the total amount of fissions at the CHOOZ and Bugey-4 experiments [24]. This explicitly means that the expected number of events was computed using σ_f^{bugey} rather than $\sigma_f^{pred,old}$, thus absorbing a -1.3% difference on the overall normalization (see Table I). This also has the effect of reducing the error on the neutrino detection rate from 2.7% to 1.6% (including the uncertainty on the fission contributions f_k). Accounting for an uncertainty on off-equilibrium effects, CHOOZ quoted a final neutrino spectrum error of 1.9%. As shown above, the new values from Ref. [16] lead to an increase of $\sigma_f^{pred,new} = 1.048\ \sigma_f^{pred,old}$. With this sizeable discrepancy between measured and computed cross sections, the CHOOZ experiment cannot rely anymore on the effective cross section per fission measured at Bugey-4, assuming no-oscillation at baselines of less than a few tens of meters. We thus revise the ratio to R_{CHOOZ}=0.961 ± 0.027(stat.) ± 0.032(syst.) (see Table II), where the 3.3% systematic error now includes the 2.7% uncertainty on $\sigma_f^{pred,new}$ (See Appendix A).

A crude analysis of the impact of Ref. [16] on Palo Verde data [31] leads to the modification of the average ratio of detected versus expected $\bar{\nu}_e$ by roughly −3.5%, leading to $R_{PaloVerde} = 0.975 \pm 0.023(\text{stat.}) \pm 0.055(\text{syst.})$. We also note that Palo Verde's uncertainty would increase from 5.3% in Ref. [31] to 5.6% according to our prescription.

IV. THE REACTOR ANTINEUTRINO ANOMALY

A. Rate information

Up to now we independently studied the results of the main reactor neutrino experiments using a new value of the cross section per fission, $\sigma_f^{pred,new}$. The observed event rates to predicted event rates ratios, $R = N_{obs}/N_{pred}$, are summarized in Table II. We observe a general systematic shift more or less significantly below unity. These reevaluations unveil a new *reactor antineutrino anomaly*, clearly illustrated in Figure 4, but still to be explained. In order to quantify the statistical significance of the anomaly we can compute the weighted average of the ratios of expected over predicted rates, for all short baseline reactor neutrino experiments (including their possible correlations).

We consider the following experimental rate information: Bugey-4 and ROVNO, the three Bugey-3 experiments, the three Goesgen experiments and the ILL experiment, the three Krasnoyarsk experiments, Palo Verde, and CHOOZ. $\overrightarrow{\mathrm{R}}$ is the corresponding vector of ratios of observed to predicted events. We assume the most generally used value, 2.7%, as the systematic uncertainty on the reactor antineutrino rate. This includes the S_{tot} uncertainty and the f_k uncertainties. We correlated this error between all reactor neutrino experiments. We considered the ratios and relative errors gathered in Table II. In order to account for the experimental correlations we fully correlate the experimental errors of Bugey-4 and ROVNO, of the three Goesgen and the ILL experiments, and finally of the 3 Krasnoyarsk experiments. We only used the error budget published by the collaborations, without any renormalization. We then obtain the reactor experiment covariance matrix W:

$$\begin{pmatrix}
0.0900 & 0.0900 & 0.0729 & 0.0729 & 0.0729 & 0.0729 & 0.0729 & 0.0729 & 0.0729 & 0.0729 & 0.0729 & 0.0729 & 0.0729 & 0.0729 \\
0.0900 & 0.1520 & 0.0729 & 0.0729 & 0.0729 & 0.0729 & 0.0729 & 0.0729 & 0.0729 & 0.0729 & 0.0729 & 0.0729 & 0.0729 & 0.0729 \\
0.0729 & 0.0729 & 0.2516 & 0.2500 & 0.2500 & 0.0729 & 0.0729 & 0.0729 & 0.0729 & 0.0729 & 0.0729 & 0.0729 & 0.0729 & 0.0729 \\
0.0729 & 0.0729 & 0.2500 & 0.2600 & 0.2500 & 0.0729 & 0.0729 & 0.0729 & 0.0729 & 0.0729 & 0.0729 & 0.0729 & 0.0729 & 0.0729 \\
0.0729 & 0.0729 & 0.2500 & 0.2500 & 1.9924 & 0.0729 & 0.0729 & 0.0729 & 0.0729 & 0.0729 & 0.0729 & 0.0729 & 0.0729 & 0.0729 \\
0.0729 & 0.0729 & 0.0729 & 0.0729 & 0.0729 & 0.4176 & 0.3600 & 0.3600 & 0.3600 & 0.0729 & 0.0729 & 0.0729 & 0.0729 & 0.0729 \\
0.0729 & 0.0729 & 0.0729 & 0.0729 & 0.0729 & 0.3600 & 0.4176 & 0.3600 & 0.3600 & 0.0729 & 0.0729 & 0.0729 & 0.0729 & 0.0729 \\
0.0729 & 0.0729 & 0.0729 & 0.0729 & 0.0729 & 0.3600 & 0.3600 & 0.5809 & 0.3600 & 0.0729 & 0.0729 & 0.0729 & 0.0729 & 0.0729 \\
0.0729 & 0.0729 & 0.0729 & 0.0729 & 0.0729 & 0.3600 & 0.3600 & 0.3600 & 0.9106 & 0.0729 & 0.0729 & 0.0729 & 0.0729 & 0.0729 \\
0.0729 & 0.0729 & 0.0729 & 0.0729 & 0.0729 & 0.0729 & 0.0729 & 0.0729 & 0.0729 & 0.2598 & 0.1722 & 0.1722 & 0.0729 & 0.0729 \\
0.0729 & 0.0729 & 0.0729 & 0.0729 & 0.0729 & 0.0729 & 0.0729 & 0.0729 & 0.0729 & 0.1722 & 4.1323 & 0.1722 & 0.0729 & 0.0729 \\
0.0729 & 0.0729 & 0.0729 & 0.0729 & 0.0729 & 0.0729 & 0.0729 & 0.0729 & 0.0729 & 0.1722 & 0.1722 & 0.1722 & 0.0729 & 0.0729 \\
0.0729 & 0.0729 & 0.0729 & 0.0729 & 0.0729 & 0.0729 & 0.0729 & 0.0729 & 0.0729 & 0.0729 & 0.0729 & 0.0729 & 0.3721 & 0.0729 \\
0.0729 & 0.0729 & 0.0729 & 0.0729 & 0.0729 & 0.0729 & 0.0729 & 0.0729 & 0.0729 & 0.0729 & 0.0729 & 0.0729 & 0.0729 & 0.1849
\end{pmatrix} 10^{-2}. \quad (7)$$

All the above-mentioned experiments published ratios of measured to expected event rates. While the rates themselves can be considered to follow Gaussian distributions, the ratio of two Gaussian variables does not. This may lead to overestimating the statistical significance of the deviation of the ratios from unity, as was pointed out by James in response to a paper by Reines et al. [53]. In order to check our results, we performed simple Monte-Carlo simulations: each experiment's observed and expected rates were simulated within their quoted errors, including the correlations between experiments shown in the covariance matrix W.

We then calculated the best-fit average ratio $r_{\rm best}$ for each simple Monte-Carlo experiment by minimizing the χ^2 function with respect to r:

$$\left(r - \overrightarrow{\rm R}\right)^T W^{-1} \left(r - \overrightarrow{\rm R}\right), \qquad (8)$$

and obtained the distribution of $r_{\rm best}$ (we note μ its mean in the following paragraph). We found that it is almost Gaussian, but with slightly longer tails, which we decided to take into account in our calculations (in contours that appear later in this article we enlarged the error bars). If we consider only experiments with baselines < 100 m to get rid of a possible (θ_{13}, Δm^2_{31}) driven oscillation effect at Palo Verde or CHOOZ, we obtain the mean ratio μ=0.979±0.029 with the old antineutrino spectra, and the fraction of simple Monte-Carlo experiments with $r \geq 1$ is 23.2% (-0.73σ from expectation). With the new antineutrino spectra, we obtain μ=0.937±0.027, and the fraction of simple Monte-Carlo experiments with $r \geq 1$ is 1.58%, corresponding to a -2.14σ effect (while a simple calculation assuming normality would lead to -2.34σ). Clearly the new spectra induce a statistically significant deviation from the expectation. Keeping all our corrections on the neutron mean life and out-of-equilibrium effects but using the old reference spectra $S_k(E_\nu)$ we would get an average ratio of μ=0.970±0.029, only 1.0 sigma below its (old) expectation.

In the following we define an experimental cross section σ_f^{ano}= 0.937 × $\sigma_f^{pred,new}$ 10^{-43} cm^2/fission.

We will now discuss the possible explanations of this deviation from unity: an erroneous prediction of the antineutrino flux from the reactors, or a correlated artifact in the experiments, or a real physical effect if both previous cases are excluded.

Due to the importance of the antineutrino rate increase we suggest that independent nuclear physics groups should perform similar computations. We also consider that new measurements of the electron spectra of irradiated fissile isotopes would help clarifying the anomaly. All cross sections of reactions used for the absolute and relative normalizations of the ILL electron spectra have been checked and found in agreement with the published values within error bars. A more complete discussion on the evaluation of the normalization of reactor antineutrino spectra based on the *ab initio* method will be published later in [38].

Assuming the correctness of $\sigma_f^{pred,new}$ the anomaly could be explained by a common bias in all reactor neutrino experiments. We note that the standard deviation of the distribution of all experimental ratios is about 1%, not taking the uncertainty on the antineutrino spectra into account. This is somewhat less than what could have been expected from the experimental error distribution.

The measurements used one of two techniques, scintillator counters and integral detectors. The Bugey-3 experiment [4] used 3 identical detection modules, each of 600 liters, filled with ^{6}Li-loaded liquid scintillator. Bugey-3 recorded 120,000 neutrino interactions. The Bugey-4 experiment [3] used the ROVNO [6] integral type detector, but increasing the antineutrino rate by a factor of three. In such detectors, based on ^{3}He-filled counters, the total number of antineutrino interactions is measured by detecting only the neutrons from reaction Eq. 3. The Goesgen experiment [5] used a detector nearly identical to the one used for the ILL neutrino experiment [2], but with the additional feature of position sensitivity. More than 10,000 neutrino events were recorded at the three detector locations. The detector contained liquid scintillator surrounded by ^{3}He-filled wire chambers for neutron detection. Both the positron and the neutron from reaction Eq. 3 were detected. Krasnoyarsk [7] used an integral detector with a scintillation section. Strong correlations exist between the three Goesgen experimental results together with the measurement at ILL. The three Bugey-3 results are also correlated with one another, as well Bugey-4 and ROVNO.

Neutrons were tagged either by their capture in metal-loaded scintillator, or in proportional counters, thus leading to two distinct systematics. As far as the neutron detection efficiency calibration is concerned, we note that different types of radioactive sources emitting sub-MeV electron neutrino were used (Am-Be, ^{252}Cf, Sb-Pu, Pu-Be).

It should be mentioned that the Krasnoyarsk and ILL experiments operated with nuclear fuel such that the difference between the real antineutrino spectrum and ^{235}U spectrum was less than 1%. They reported similar deficits to those observed at other reactors operating with a mixed fuel of ^{235}U, ^{239}Pu, ^{241}Pu and ^{238}U. Hence the anomaly cannot be associated with a single fissile isotope.

All the elements discussed above argue against a trivial bias in the experiments, but a detailed analysis of the most sensitive of them, involving the experts, would certainly improve the quantification of the anomaly.

B. Shape information

In this Section we re-analyze the Bugey-3 and ILL shape information, based on the published data [2, 4]. We will use this information for our combined analysis described in the next section.

1. Bugey-3

Based on the analysis of the shape of their energy spectra at different source-detector distances [4, 5], the Goesgen and Bugey-3 measurements require that $\Delta m^2 < 1\text{eV}^2$ for $\sin^2(2\theta) > 0.05$.

For further analysis we used Bugey-3's 40m/15m ratio data from [4] as it provides the best limit. We followed the steps outlined in [4], building the following estimator:

$$\chi^2 = \sum_{i=1}^{N=25} \left(\frac{(1+a)R^i_{th} - R^i_{obs}}{\sigma_i} \right)^2 + \left(\frac{a}{\sigma_a} \right)^2, \qquad (9)$$

where R^i_{obs} are our simulated data for Bugey from our tuned simulation and R^i_{th} are our Monte-Carlo expectation in each bin. The σ_i are the errors reported by the Bugey-3 collaboration, and a is a systematic parameter accounting for the $\sigma_a = 2\%$ uncertainty on the relative normalization at 40 m and 15 m. Figure 16 of [4] shows the 90% C.L. exclusion contour from a *raster scan* analysis with this estimator. As can be seen in figure 1, we adequately reproduce Bugey-3's results.

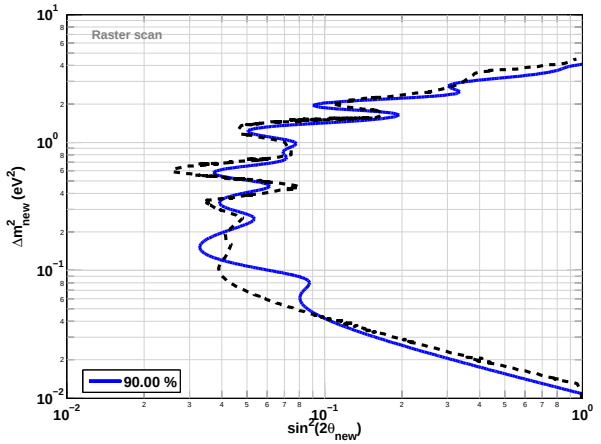

FIG. 1. 90% C.L. exclusion domains obtained in the Δm^2-$\sin^2(2\theta)$ plane from a raster scan of Bugey-3's data. Our result (continuous line) is in good agreement with the original result from [4] (dashed line), excluding oscillations such that $\Delta m^2 < 1$ eV^2 for $\sin^2(2\theta) > 0.05$.

We already note here that in section V, when combining Bugey-3's shape information with other results, we use the estimator from equation 9, but we perform a standard *global scan* (i.e. the minimization is performed over the entire $\Delta m^2, \sin^2 2\theta$ plane). We only perform a raster scan here to show our agreement with the collaboration's original analysis.

2. ILL

As already noted in Ref. [23] the data from ILL showed a spectral deformation compatible with an oscillation pattern in their measured over predicted events ratio. It should be mentioned that the parameters best fitting the data reported by the authors of Ref. [23] were $\Delta m^2 = 2.2$ eV^2 and $\sin^2(2\theta) = 0.3$.

We reanalyzed the data of Ref. [23] in order to include the ILL shape-only information in our analysis of the reactor antineutrino anomaly. We built the following shape-only estimator

$$\chi^2_{\text{ILL,shape}} = \sum_{i=1}^{N=16} \left(\frac{(1+a)R^i_{th} - R^i_{obs}}{\sigma_i} \right)^2 \qquad (10)$$

where R^i_{obs} are the measured ratios in each energy bin, and R^i_{th} are our Monte-Carlo expectation in each bin. a is a free parameter in the fit, which renders this estimator completely insensitive to any normalization information. It is therefore only sensitive to the shape of the distribution.

σ_i is the total error in each bin: we added in quadrature the statistical error and a systematic error of 11%. It was difficult to extract the magnitude of this shape-only systematic error from published information. We combined our $\chi^2_{\text{ILL,shape}}$ estimator with the rate-only estimator, and verified that with this value of the systematic, we could reproduce the ILL contours of both papers: when using $R_{ILL,80}$ we reproduced the contour in Figure 14 of Ref. [2], and when using $R_{ILL,95}$ we reproduced that of Ref. [23] which excludes the no-oscillation hypothesis at 2σ. A systematic error of 11% is consistent with figure 13 of Ref. [2]. It is also a conservative treatment of the shape-only information: with such an error the data are compatible with the no-oscillation hypothesis at 1σ. Figure 2 shows the data points from [23], along with our best fit from the shape-only estimator ($|\Delta m^2| \sim 2.3$ eV^2, $\sin^2(2\theta) \sim 0.24$), and the no-oscillation line for comparison.

V. THE FOURTH NEUTRINO HYPOTHESIS

In this section we discuss the compatibility of the reactor antineutrino anomaly with the existence of a fourth non-standard neutrino, corresponding in the flavor basis to the existence of a sterile neutrino ν_s (see [1] and references therein). The motivation is the explanation of the antineutrino deficit by an oscillation of electron neutrinos into a new neutrino state with a large Δm^2_{new} value.

For simplicity we restrict our analysis to the 3+1 four-neutrino scheme in which there is a group of three active neutrino masses separated from an isolated neutrino mass, such that $|\Delta m^2_{new}| \gg 10^{-2}$ eV^2. The latter would be responsible for very short baseline reactor neutrino oscillations. For energies above the inverse beta decay threshold and baselines of <2 km, we adopt the approx-

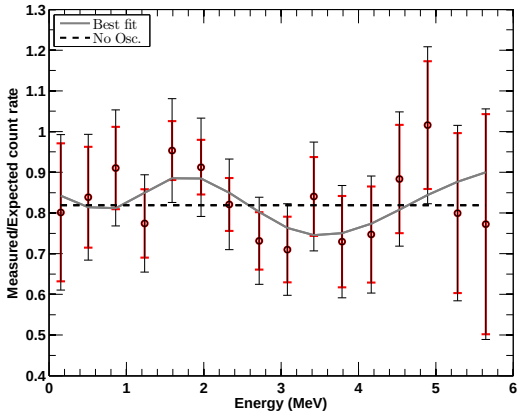

FIG. 2. Ratio of measured to expected positron energy spectra of the ILL neutrino experiment (data points extracted from [23]). We show the best fit line with oscillations, along with the no-oscillation line, from our shape-only fit. The short error bars are statistical and the longer ones include the 11% systematic error described in the text.

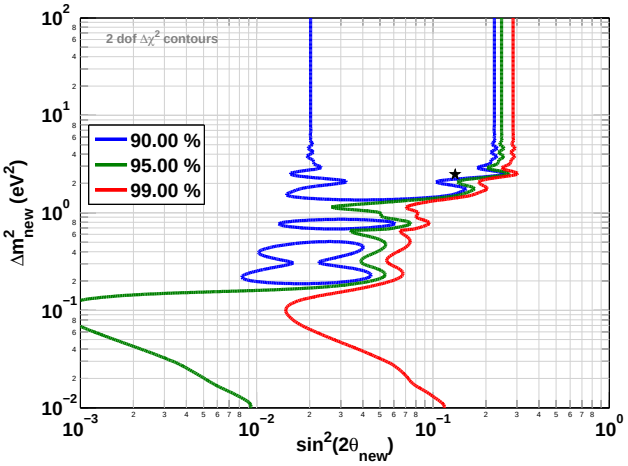

FIG. 3. Allowed regions in the $\sin^2(2\theta_{new}) - \Delta m^2_{new}$ plane obtained from the fit of the reactor neutrino data, without ILL-shape information, but with the stringent oscillation constraint of Bugey-3 based on the 40m/15 m ratios to the 3+1 neutrino hypothesis, with $\sin^2(2\theta_{13}) = 0$. The best-fit point is indicated by a star.

imated oscillation formula from Ref. [39]:

$$P_{ee} = 1 - \cos^4\theta_{new}\sin^2 2\theta_{13}\sin^2\left(\frac{\Delta m^2_{31}L}{4E_{\bar{\nu}_e}}\right) - \sin^2 2\theta_{new}\sin^2\left(\frac{\Delta m^2_{new}L}{4E_{\bar{\nu}_e}}\right). \quad (11)$$

In our analyses the well known solar driven oscillation effects are negligible. The contribution of the atmospheric driven oscillation is negligible at distances < 100 m. It is worth noting that we are not sensitive to any sterile neutrino mass hierarchy in the mass range considered.

The ILL experiment may have seen a hint of oscillation in their measured positron energy spectrum (see Section III B), but the Bugey-3 results do not point out any significant spectral distortion more than 14 m away from the antineutrino source. Hence, in a first approximation, hypothetical oscillations could be seen as an energy-independent suppression of the $\bar{\nu}_e$ rate by a factor of $0.5\sin^2 2\theta_{new,R}$, thus leading to $\Delta m^2_{new,R} \gtrsim 1$ eV^2 and accounting for Bugey-3 and Goesgen shape analyses [4, 5]. Considering the weighted averaged of all reactor experiments we get an estimate of the mixing angle, $\sin^2 2\theta_{new,R} \sim 0.13$.

Let us now fit the sterile neutrino hypothesis to the data (baselines below 2 km) by minimizing the least-squares function

$$\left(P_{ee} - \overrightarrow{\mathrm{R}}\right)^T W^{-1}\left(P_{ee} - \overrightarrow{\mathrm{R}}\right), \quad (12)$$

assuming $\sin^2(2\theta_{13}) = 0$.

Figure 3 provides the results of the fit in the $\sin^2(2\theta_{new}) - \Delta m^2_{new}$ plane, including the reactor experiment rate information as well as the 40m/15m Bugey-3 spectral shape constraint presented in Figure 1. The latter leads to stringent oscillation constraints for $|\Delta m^2_{new,R}| \leq 1$ eV^2, since no spectral distortion was observed in the ratio 40m/15m. The fit to the data indicates that $|\Delta m^2_{new,R}| > 0.2$ eV^2 (95%) and $\sin^2(2\theta_{new,R}) \sim 0.1$. Note that if we include a non-zero value of $\sin^2(2\theta_{13})$, as large as the 90% C.L. CHOOZ bound [10], the contours presented in Figure 3 are only marginally affected.

Ignoring the reactor anomaly leads to an ambiguous interpretation of the ∼1-2 km baseline experiment results constraining θ_{13}. As an example we compare the following two hypotheses: the 3 neutrino mixing scenario with $\sin^2(2\theta_{13}) = 0.06$ for instance and the 3+1 neutrino mixing scenario, taking $\sin^2(2\theta_{13}) = 0$, $\sin^2(2\theta_{new,R}) = 0.16$ and $|\Delta m^2_{new,R}| > 1$ eV^2 (best fit values of the combined fit shown on Figure 7) . Figure 4 displays the data together with the two hypotheses. The red line represent the three active neutrino hypothesis, considering reactor neutrino rates until the CHOOZ baseline. The goodness-of-fit of the 3 neutrino mixing hypothesis, defined here as the p-value, is 17% (18.7/14 degrees of freedom). The blue line illustrates the 3+1 neutrino mixing scenario with a large $|\Delta m^2_{new,R}|$=2.4 eV^2, leading to a goodness-of-fit of 66% (11.3/14 degrees of freedom). We note a tension between the data and the three active neutrino flavor hypothesis, again illustrating the anomaly. Clear preference is given to the 3+1 neutrino hypothesis since $\Delta\chi^2 \gtrsim 7$. A similar computation with the former reference spectra would lead to goodness-of-fits of 30% in both cases. This illustrates the impact of our reanalysis with the new antineutrino spectra, updated neutron mean lifetime, and off-equilibrium effects.

At this stage it is tempting to consider the previously

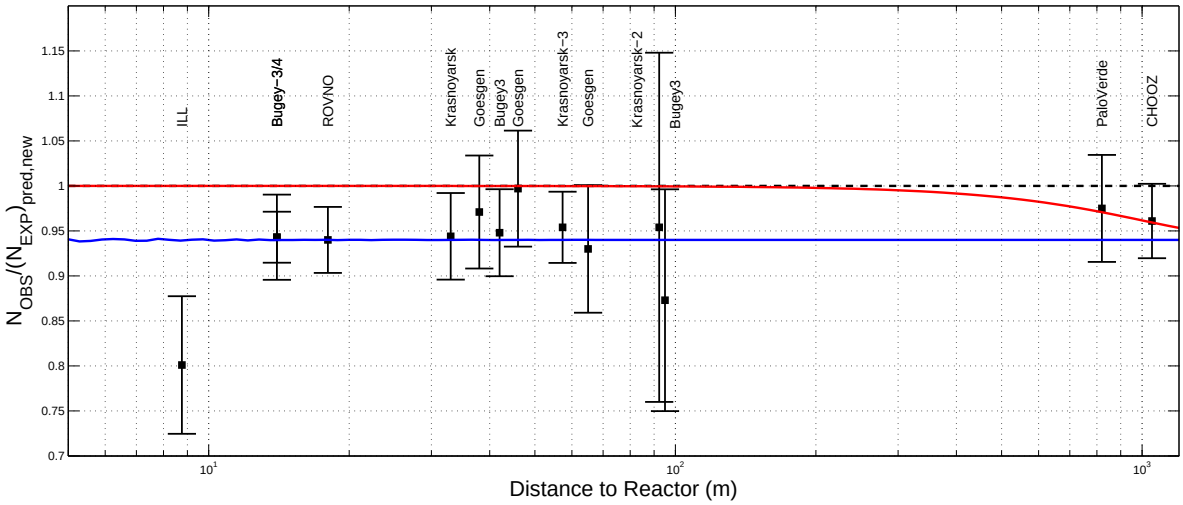

FIG. 4. Illustration of the short baseline reactor antineutrino anomaly. The experimental results are compared to the prediction without oscillation, taking into account the new antineutrino spectra, the corrections of the neutron mean lifetime, and the off-equilibrium effects. Published experimental errors and antineutrino spectra errors are added in quadrature. The mean averaged ratio including possible correlations is 0.937±0.027. The red line shows a 3 active neutrino mixing solution fitting the data, with $\sin^2(2\theta_{13}) = 0.06$. The blue line displays a solution including a new neutrino mass state, such as $|\Delta m^2_{new,R}| \gg 1$ eV^2 (for illustration) and $\sin^2(2\theta_{new,R})$=0.16.

noted anomalies affecting other short baseline electron neutrino experiments Gallex, Sage and MiniBooNE, reviewed in Ref. [43]. Our goal is to quantify the compatibility of those anomalies.

We first reanalyzed the Gallex and Sage calibration runs with ^{51}Cr and ^{37}Ar radioactive sources emitting ∼1 MeV electron neutrinos. [44], following the methodology developed in Ref. [43, 45]. However we decided to include possible correlations between these four measurements in this present work. Details are given in in Appendix B. This has the effect of being slightly more conservative, with the no-oscillation hypothesis disfavored at 97.73% C.L., instead of 98% C.L in Ref. [43]. Gallex and Sage observed an average deficit of $R_G = 0.86 \pm 0.05 (1\sigma)$. Considering the hypothesis of ν_e disappearance caused by short baseline oscillations we used Eq. (11), neglecting the Δm^2_{31} driven oscillations because of the very short baselines of order 1 meter. Fitting the data leads to $|\Delta m^2_{new,G}| > 0.3$ eV^2 (95%) and $\sin^2(2\theta_{new,G}) \sim 0.26$. Combining the reactor antineutrino anomaly with the Gallium anomaly gives a good fit to the data and disfavors the no-oscillation hypothesis at 99.7% C.L. Allowed regions in the $\sin^2(2\theta_{new}) - \Delta m^2_{new}$ plane are displayed in Figure 5 (left). The associated best-fit parameters are $|\Delta m^2_{new,R\&G}| > 0.7$ eV^2 (95%) and $\sin^2(2\theta_{new,R\&G}) \sim 0.16$.

We then reanalyzed the MiniBooNE electron neutrino excess assuming the very short baseline neutrino oscillation explanation of Ref. [43]. Details of our reproduction of the latter analysis are provided in Appendix B. The best fit values are $|\Delta m^2_{new,MB}| = 1.9$ eV^2 and $\sin^2(2\theta_{new,MB}) \sim 0.2$, but are not significant at 95% C.L. The no-oscillation hypothesis is only disfavored at the level of 72.4% C.L., less significant than the reactor and gallium anomalies. Combining the reactor antineutrino anomaly with our MiniBooNE reanalysis leads to a good fit with the sterile neutrino hypothesis and disfavors the absence of oscillations at 97.5% C.L., dominated by the reactor experiments' data. Allowed regions in the $\sin^2(2\theta_{new}) - \Delta m^2_{new}$ plane are displayed in Figure 5 (right). The associated best-fit parameters are $|\Delta m^2_{new,R\&MB}| > 1.4$ eV^2 (95%) and $\sin^2(2\theta_{new,R\&MB}) \sim 0.1$.

Experiment(s)	$\sin^2(2\theta_{new})$	$\lvert\Delta m^2_{new}\rvert$ (eV^2)	C.L. (%)
Reactors (no ILL-S,R*)	0.02-0.23	>0.2	95.0
Gallium (G)	0.06-0.4	>0.3	97.7
MiniBooNE (M)	—	—	72.4
ILL-S	—	—	68.2
R* + G	0.07-0.24	>1.5	99.7
R* + M	0.04-0.23	>1.4	97.5
R* + ILL-S	0.04-0.23	>2.0	97.1
ALL	0.06-0.25	>2.0	99.93

TABLE III. Best fit parameter intervals or limits at (95%) for ($\sin^2(2\theta_{new})$, Δm^2_{new}) and significance of the sterile neutrino oscillation hypothesis in %, for different combinations of the reactor experiment rates only (R*), the ILL-energy spectrum information (ILL-S), the Gallium experiments (G), and MiniBooNE-ν (M) re-analysis of Ref. [43].

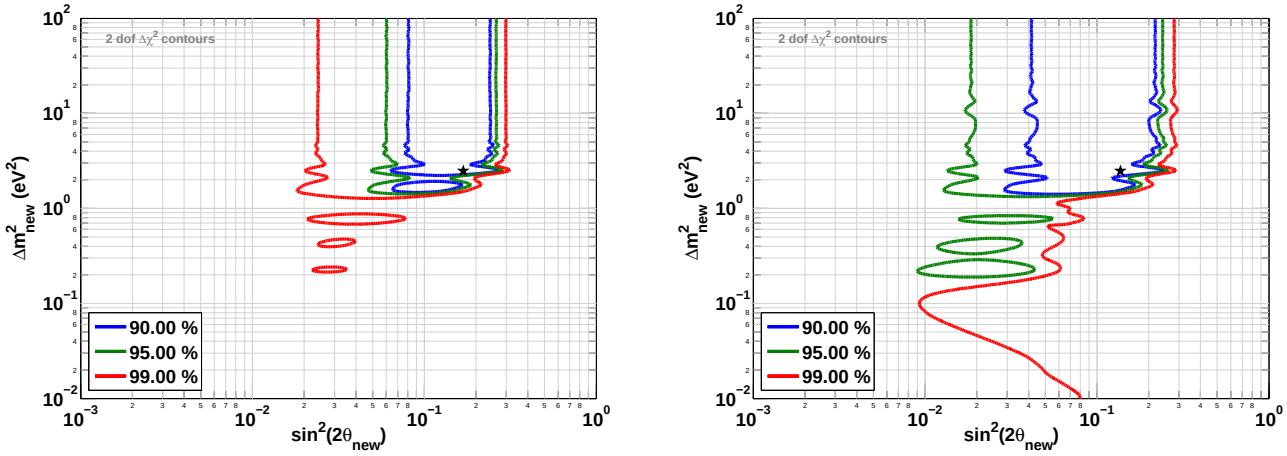

FIG. 5. Allowed regions in the $\sin^2(2\theta_{new}) - \Delta m^2_{new}$ plane obtained from the fit of the reactor neutrino data to the 3+1 neutrino hypothesis, with $\sin^2(2\theta_{13}) = 0$. The left panel is the combination of the reactors and the Gallium experiment calibration results with ^{51}Cr and ^{37}Ar radioactive sources. The right panel is the combination of the reactors and our reanalysis of the MiniBooNE data following the method of Ref. [43]. In both cases the ILL energy spectrum information is not included.

Our ILL re-analysis, including only the energy spectrum shape, leads to the allowed regions in the $\sin^2(2\theta_{new}) - \Delta m^2_{new}$ plane presented in Figure 6. We notice a hint of neutrino oscillations such that $|\Delta m^2_{new,ILL-shape}| > 1\text{eV}^2$ and $\sin^2(2\theta_{new,ILL-shape}) \sim 0.2$, in agreement with our fourth neutrino hypothesis, but still compatible with the absence of oscillations at the 1σ level. Figure 2 is our reproduction of the illustration 3 of Ref. [2]; we superimposed the oscillation pattern that would be induced by neutrino oscillations at our best fit (combined analysis). The ILL positron spectrum is thus agreement with the oscillation parameters found independently in our re-analyses, mainly based on rate information. Due to the difference of systematic effects for rate and shape analysis this coincidence is in favor of a true physical effect rather than an experimental anomaly. As a cross check we performed a Monte-Carlo simulation of the ILL and Bugey-3 experiments, including the finite spatial extension of the nuclear reactors and the ILL and Bugey-3 detectors. We found that the small dimensions of the ILL nuclear core lead to small corrections of the oscillation pattern imprinted on the positron spectrum. However the large extension of the Bugey nuclear core is sufficient to wash out most of the oscillation pattern at 15 m. This explains the absence of shape distortion in the Bugey-3 experiment.

Table III summarizes all the results of our fits of reactor, gallium, and MiniBooNE-ν data to the sterile neutrino oscillation hypothesis. We observe that all the data sets taken separately are very consistent with one another, pointing to very similar oscillation parameters. We thus performed a global fit to all available data.

The no-oscillation hypothesis is disfavored at 99.93% C.L. The significance is dominated by the gallium and reactor data. Allowed regions in the $\sin^2(2\theta_{new}) - \Delta m^2_{new}$ plane are displayed in Figure 7, together with the marginal $\Delta\chi^2$ profiles for $|\Delta m^2_{new}|$ and $\sin^2(2\theta_{new})$. The combined fit leads to a best-fit solution at $|\Delta m^2_{new}| > 2.4 \pm 0.2$ eV^2 and $\sin^2(2\theta_{new}) = 0.17 \pm 0.08$ (95%) but higher values of $|\Delta m^2_{new}| > 1.5$ eV^2 are allowed by the data, at 95%. We remark that a solution is slightly favored around the best fit value, at $|\Delta m^2_{new}| = 2.35 \pm 0.1$ eV^2 (68%) and $\sin^2(2\theta_{new}) = 0.165 \pm 0.04$ (68%). An embryo of possible consequences of this result will be discussed in Section VIII.

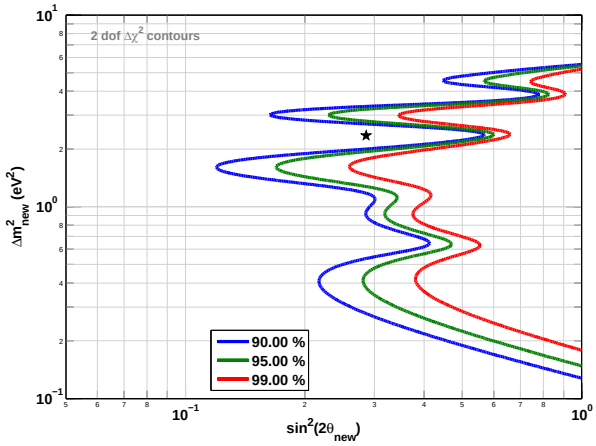

FIG. 6. Allowed regions in the $\sin^2(2\theta_{new}) - \Delta m^2_{new}$ plane obtained from a fit of the ILL energy spectrum shape only. The best fit value reported by the authors of Ref. [23] is very close to our best fit, at $|\Delta m^2_{new}| \sim 2$ eV^2, but it is worth noting its poor statistical significance, compatible with the absence of oscillations at the 1σ level. The best-fit point is indicated by a star.

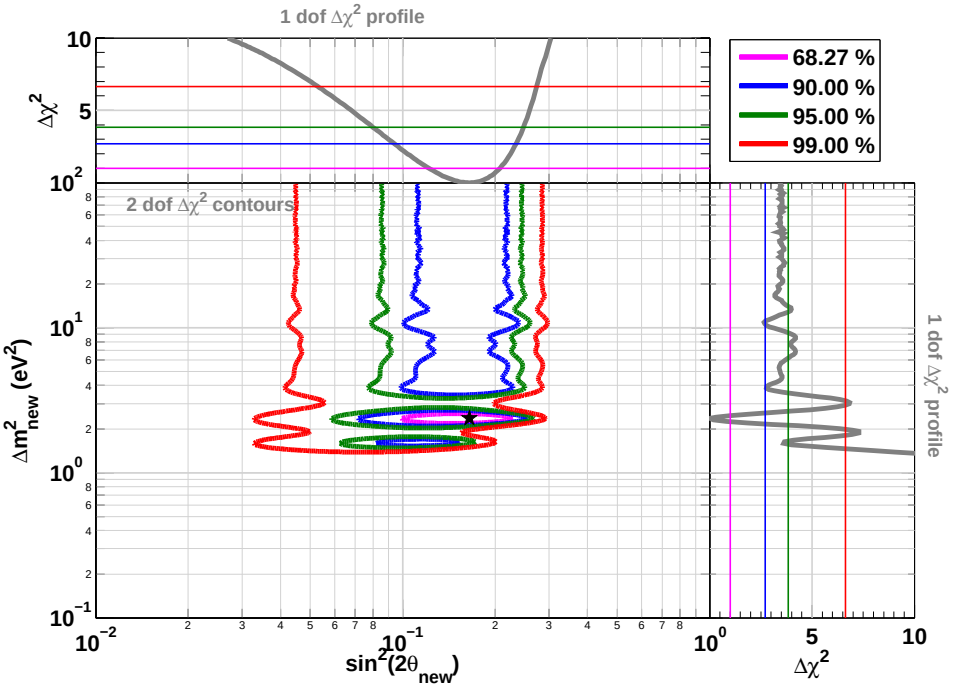

FIG. 7. Allowed regions in the $\sin^2(2\theta_{new}) - \Delta m^2_{new}$ plane from the combination of reactor neutrino experiments, Gallex and Sage calibration sources experiments, MiniBooNE reanalysis of Ref. [43], and the ILL-energy spectrum distortion. The data are well fitted by the 3+1 neutrino hypothesis, while the no-oscillation hypothesis is disfavored at 99.93% C.L. The marginal $\Delta\chi^2$ profiles for $|\Delta m^2_{new}|$ and $\sin^2(2\theta_{new})$ (1 dof) lead to the constraints, $|\Delta m^2_{new}| > 1.5$ eV^2 (95%) and $\sin^2(2\theta_{new}) = 0.17 \pm 0.08$ (95%). The best fit value is at $|\Delta m^2_{new}| = 2.35 \pm 0.1$ eV^2 (68%) and $\sin^2(2\theta_{new}) = 0.165 \pm 0.04$ (68%).

VI. REVISION OF THE CONSTRAINTS ON θ_{13}

In this section we discuss the impact of our revision of the results of the short baseline (< 100 m) reactor experiments on the constraints on the θ_{13} mixing angle from CHOOZ [10], KamLAND [14], and by their combination. Considering the hypothesis of the existence of a non-standard neutrino, the results depend on the choice of the cross section per fission used to normalize the predicted antineutrino rate, as well as of the neutrino oscillation scheme used in the analysis, including a non-standard neutrino or not. Assuming the correctness of the neutrino experiments (detected rate) we show that constraints on θ_{13} could be derived by using $\sigma_f^{pred,ano}$ and the three-active neutrino scenario.

A. CHOOZ

We first reproduced CHOOZ background-subtracted results and Monte-Carlo using Ref. [10]. We used the converted neutrino spectra from ILL electron data [18, 27, 28], using the parameterization from Ref. [34], and the V-A cross section from [26], normalized to the Bugey-4 value as was done in Ref. [10]. Long-lived fission product contributions were also taken into account (at 300 days of irradiation). As in Ref. [10], we accounted for a 2.7% systematic error on the overall normalization and a 1.1% error on the energy scale, along with a bin-to-bin uncorrelated uncertainty describing the uncertainty of the neutrino spectrum. Using the original ILL neutrino converted spectra, with the σ_f^{bugey} cross-section we could roughly reproduce the exclusion limit from Ref. [10] (black dashed line on Figure 8) to acceptable precision (red line on Figure 8)in the relevant Δm^2_{31} range, although we could not fully imitate every step in the published analysis. In particular we did not use the same statistical treatment, using only a global scan while the CHOOZ Collaboration used the Feldman-Cousins unified approach to extract the confidence interval.

Let us now revisit the CHOOZ results using the new antineutrino spectra in the three active neutrino framework. We perform the same analysis as before, but computing the expected number of events based on $\sigma_f^{pred,new}$ and its error. σ_α was thus increased to 3.3% to account for this effect. This leads to a new exclusion limit, $\sin^2(2\theta_{13}) < 0.25$ (1 dof) at 90% C.L. for $\Delta m^2_{31} = 2.4\,10^{-3}$ eV^2. The corresponding exclusion contour is displayed as the blue line on Figure 8. In this approach we make use of $\sigma_f^{pred,new}$ and attribute the slight deficit of $\bar{\nu}_e$ at CHOOZ to a θ_{13} driven oscillation, such that $\sin^2(2\theta_{13}) = 0.10^{+0.07}_{-0.08}$. However this result only holds

within the three active neutrino mixing framework, under the hypothesis of no-oscillation at very short baselines. But in Section IV we pointed out an anomaly affecting the short baseline reactor neutrino experiment results. In the scenario discussed above with a new neutrino (m_{new}, θ_{new}) we generate oscillations driven by a large $|\Delta m^2_{new}| \gg \Delta m^2_{31}$. In this case CHOOZ measured a combination of the oscillation driven by $(\Delta m^2_{new}, \theta_{new})$ and $(\Delta m^2_{31}, \theta_{13})$. A comprehensive 3+1 neutrino analysis would thus be mandatory to constrain θ_{13} using the new normalization based on $\sigma_f^{pred,new}$, but we will see next that another approach may be used.

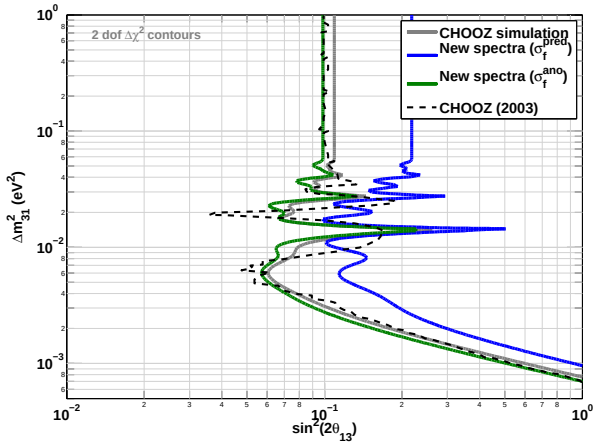

FIG. 8. Our simulation (gray line) roughly reproduces the published CHOOZ exclusion limit [10] represented by the black dashed line. We obtain the blue contour by normalizing the expected no-oscillation antineutrino rate to $\sigma_f^{pred,new}$ and analyzing the data using the three active neutrino oscillations scheme. We then normalize the expected antineutrino event rate to σ_f^{ano} to account for possible neutrino oscillations at very short baselines, leading to the green contour. This provides our new constraint on $\sin^2(2\theta_{13})$, accounting for the reactor antineutrino anomaly.

As a matter of fact the CHOOZ experiment used σ_f^{bugey} instead of $\sigma_f^{pred,new}$. The collaboration justified making use of σ_f^{bugey} because of the good agreement with $\sigma_f^{pred,old}$. With our revision of σ_f^{pred} this justification does not hold anymore in the 3 neutrino oscillation framework. But it turns out that if we assume non-standard neutrino oscillations in the large $|\Delta m^2_{new}| \gg 0.1$ eV^2 regime (no spectral distortion), the normalization of CHOOZ using $\sigma_f^{bugey} \sim \sigma_f^{ano}$ leads to an estimator of $\sin^2(2\theta_{13})$ getting rid of a possible degeneracy with $\sin^2(2\theta_{new})$. CHOOZ's strategy was indeed to absorb possible errors in rate predictions, but this methodology holds as well for constraining θ_{13} on top of an additional short baseline averaged oscillations.

Thus a pragmatic approach for constraining θ_{13} from CHOOZ data is the use of the measured weighted averaged cross section of all experiments < 100m, σ_f^{ano}. This leads to a new exclusion limit, $\sin^2(2\theta_{13}) < 0.09$ (1 dof) at 90% C.L. for $\Delta m^2_{31} = 2.4\,10^{-3}$ eV^2, slightly lower than the CHOOZ's published value [10].

B. KamLAND

In this section we reevaluate the KamLAND constraint on θ_{13} in light of the reactor antineutrino anomaly.

Unlike in the original CHOOZ analysis from [10], the KamLAND $\bar{\nu}_e$ energy spectrum is calculated using $\sigma_f^{pred,old}$ based on Ref. [18, 27]. But the spectral uncertainty is evaluated from Ref. [3], including off-equilibrium effects. In this case the propagation of the Bugey-4 error on σ_f^{pred} only has a marginal impact since it is not among the dominant systematics.

We first reproduced KamLAND results and Monte-Carlo to a very good accuracy exploiting Ref. [14] as well as publicly available information [33]. We used the parameterization of Ref. [34] for S_{tot}, and included off-equilibrium corrections according to Ref. [16]. Special care was taken to include all published backgrounds, known antineutrino sources, especially Korean power reactors, and geoneutrinos. We tuned our simulation to reproduce KamLAND's Monte-Carlo with and without neutrino oscillations (adjusting each effective power of the Japanese power plants). In both cases our simulation agrees with that of KamLAND to better than 1% in the 1.5-6.5 MeV range.

Confidence levels in the $(\tan^2\theta_{12}, \sin^2\theta_{13})$ plane were obtained by minimizing the generic χ^2 function:

$$\chi^2 = \sum_i \left(\frac{Y_i - N_i(\alpha,\beta)}{Y_i} \right)^2 + \beta^T W^{-1} \beta \qquad (13)$$

where the Y_i are our simulated data tuned to KamLAND's Monte-Carlo [14]. The free parameters are α (θ_{12}, θ_{13}, Δm^2_{21} and geo-ν rate), and the nuisance parameters, β, which are the systematics quoted in Ref. [14]. The $N_i(\alpha,\beta)$ are our simulation model for all the free parameters. The W^{-1} matrix contains all the systematic uncertainties quoted in Ref. [34].

Figure 9 demonstrates that we could reproduce the best fit and the confidence contours of KamLAND [14] with good accuracy. With the original reactor neutrino spectra S_{tot}, we obtain a good agreement with KamLAND's published results [14]. Changing the reference spectra S_{tot} according to Ref. [16], the best fit values and uncertainties on $\tan^2\theta_{12}$ and Δm^2_{21} are unaffected in a three active neutrino, oscillations framework, but the $\sin^2(2\theta_{13})$ central value is shifted upwards to $\sin^2(2\theta_{13}) = 0.2^{+0.14}_{-0.14}$, consistent with zero at 1.4σ. The new 90% C.L. limit on $\sin^2(2\theta_{13})$ would therefore increase to 0.41 (1 dof), marginalizing over the other fit parameters.

However, as in the case of CHOOZ discussed above, these results do not take into account the reactor antineutrino anomaly at short baselines. In the 3+1 neu-

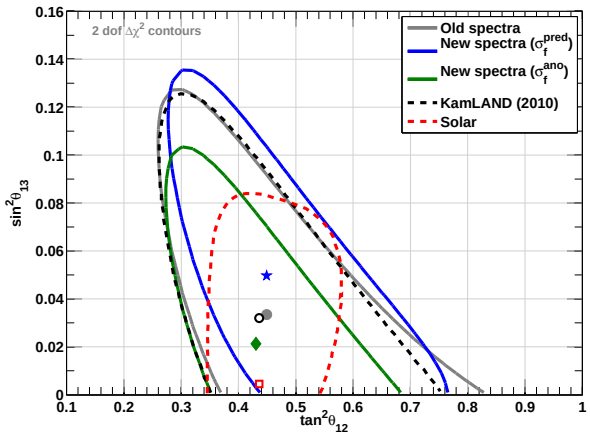

FIG. 9. Our simulation (gray line, gray disk) reproduces the published 95% C.L. KamLAND inclusion contour [14] represented by the black dashed line (black circle). We obtain the blue contour (star) by normalizing the expected no-oscillation antineutrino rate to $\sigma_f^{pred,new}$ and analyzing the data using the three active neutrino oscillations scheme. We then normalize the expected antineutrino event rate using σ_f^{ano} to account for possible neutrino oscillations at very short baselines, leading to the green contour (diamond). This provides our new constraints in the $\tan^2(\theta_{12})$-$\sin^2(\theta_{13})$ plane, accounting for the reactor antineutrino anomaly. We note that the slight tension pulling-out the $\sin^2(\theta_{13})$ best-fit values of solar (red square) and reactor data is reduced in our scenario.

trino oscillation framework, the whole effect induced by the normalization shift is absorbed by the new oscillation at very short baselines, driven by Δm^2_{new}. Normalizing KamLAND's data to σ_f^{ano} leads to an estimator revising the constraint on θ_{13} using the three-active neutrino oscillation framework, such that $\sin^2(2\theta_{13})$ <0.31 (1 dof) at 90% C.L. for $\Delta m^2_{31} = 2.4\,10^{-3}$ eV^2.

C. Combining CHOOZ and KamLAND

In sections VI A and VI B we separately revisited the CHOOZ and KamLAND results. Here, we first voluntarily ignore the reactor antineutrino anomaly at short baselines. We thus normalize both CHOOZ and KamLAND with $\sigma_f^{pred,new}$. Combining these two results leads to a best-fit value of $\sin^2(2\theta_{13}) = 0.12^{+0.06}_{-0.06}$, barely consistent with a null value of θ_{13}. The left panel of Figure 10 shows the $\Delta\chi^2$ profiles for CHOOZ (green), KamLAND (blue), and for their combination (red), as a function of $\sin^2(2\theta_{13})$, marginalizing over the other parameters. In this scenario the revised limit is $\sin^2(2\theta_{13}) < 0.22$ at 90% C.L (1 dof), for the estimation of θ_{13} only, for $\Delta m^2_{31} = 2.4\,10^{-3}$ eV^2. These results are consistent with analyses of various data sets indicating a 'hint' for a non-zero θ_{13}, reviewed in [15]. This is explained by the increase of the predicted event rate at CHOOZ and KamLAND which is attributed to θ_{13}, only, in the three neutrino oscillations framework.

	$\sigma_f^{pred,new}$		σ_f^{ano}	
Re-analysis	Best fit$^{+1\sigma}_{-1\sigma}$	90% C.L.	Best fit$^{+1\sigma}_{-1\sigma}$	90% C.L.
KamLAND	$0.20^{+0.14}_{-0.14}$	< 0.41	$0.07^{+0.14}_{-0.14}$	< 0.31
CHOOZ	$0.10^{+0.08}_{-0.08}$	< 0.25	$-0.04^{+0.08}_{-0.08}$	< 0.09
Combined	$0.12^{+0.06}_{-0.06}$	< 0.22	$-0.02^{+0.07}_{-0.07}$	< 0.09

TABLE IV. Best-fit values for $\sin^2(2\theta_{13})$ and 1σ errors, considering two possible normalizations with $\sigma_f^{pred,new}$ or σ_f^{ano}. Limits are given for a 1 dof parameter estimation.

But the previous estimation does not take into account the reactor antineutrino anomaly. Let us now consider that both CHOOZ and KamLAND are normalized with σ_f^{ano}, in order to constrain θ_{13} using a three active neutrino oscillation framework. The right panel of Figure 10 shows the $\Delta\chi^2$ profiles for CHOOZ (green), KamLAND (blue), and for their combination (red), computed as before. In this scenario the best fit is at $\sin^2(2\theta_{13}) = -0.02^{+0.07}_{-0.07}$. This lower best fit value is due to the fact that we predict fewer antineutrinos at CHOOZ and KamLAND, some of them having already oscillated into non-standard neutrinos. This leads to our revised constraint, $\sin^2(2\theta_{13})$ <0.095 at 90% C.L. (1 dof) for $\Delta m^2_{31} = 2.4\,10^{-3}$ eV^2. Results are summarized in Table IV.

We conclude that the hint for a non zero value of θ_{13} discussed in Ref. [15] vanishes if one normalizes CHOOZ's and KamLAND's predicted antineutrino rates to σ_f^{ano}. Furthermore we notice that the slight tension affecting the $\sin^2(\theta_{13})$ best-fit values of solar and reactor data [15] is reduced in our scenario involving a non-standard neutrino such that $\Delta m^2_{new} \gg \Delta m^2_{31}$.

A full analysis of the data based on non-standard neutrino oscillation models would lead to more accurate results, beyond the scope of this article.

D. Daya Bay, Double Chooz, and RENO

Three new reactor neutrino oscillation experiments, Daya Bay [11], Double Chooz [12], and RENO [13] will soon be coming online to significantly improve our knowledge of reactor antineutrino rates at various baselines.

Among these experiments Double Chooz is the only one to operate a first phase without a near detector. The evidence for a reactor antineutrino anomaly triggers the discussion of the choice of the cross section per fission to be used for constraining θ_{13}, $\sigma_f^{pred,new}$ or σ_f^{ano}, as well as its associated uncertainty.

Straightforwardly using $\sigma_f^{pred,new}$ in the three neutrino oscillation framework to interpret a hypothetical antineutrino deficit at Double Chooz would could to an overes-

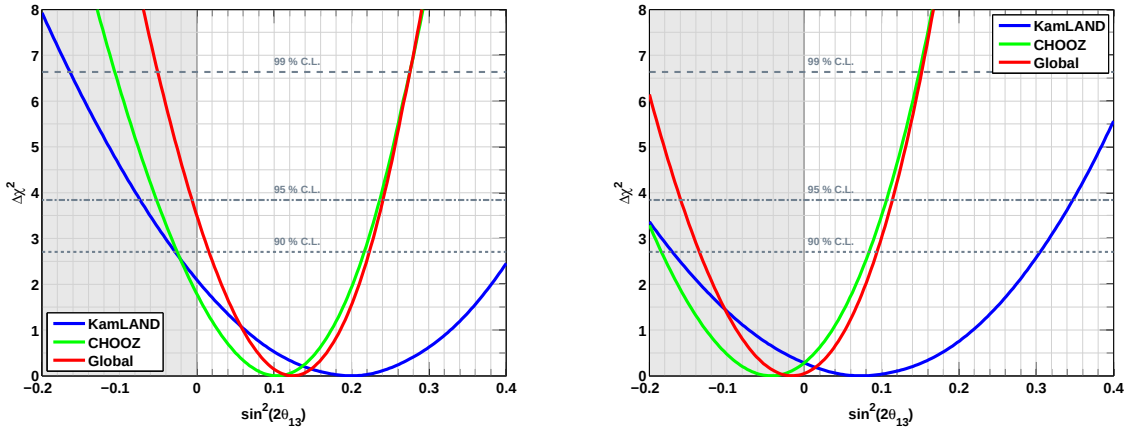

FIG. 10. Dependence of $\Delta\chi^2$ on $\sin^2(2\theta_{13})$ for CHOOZ (green), KamLAND (blue), and their combination (red). Comparing the data with the excess in expected event rate predicted using $\sigma_f^{pred,new}$ leads to an increase of the best-fit value of $\sin^2(2\theta_{13})$, in the three active neutrino oscillations framework (left). The normalization of the expected event rate with σ_f^{ano} allows to absorb the reactor antineutrino anomaly observed at very short baseline, leading to our revised constraints on $\sin^2(2\theta_{13})$.

timation of θ_{13}, which could fake a discovery. But if the sterile neutrino oscillation hypothesis discussed in this paper is proven, the use of $\sigma_f^{pred,new}$ would be possible in active+sterile neutrino oscillation frameworks. In that case the 2.7% error budget of the antineutrino spectra should be used. Assuming the average experimental results of reactor neutrino are correct, using σ_f^{ano} has the advantage to absorb either a antineutrino flux miscalculation, or a physical neutrino deficit at very short baselines, leading to a conservative constraint on θ_{13}. The error budget could then be taken as the weighted standard deviation of the short baseline experiments, 1.0%, though not representative of the experimental error distribution, pointing out a non understood covariance.

This choice is however not relevant for experiments running with a multi-detector configuration, absorbing part of the uncertainty of the reactor antineutrino fluxes, depending on the setup. Even in the hypothetical case of antineutrino oscillation at very short baselines the sensitivities of Daya Bay, Double Chooz, and RENO should be marginally affected because of the large allowed values of Δm^2_{new}. However this statement should be checked based on detailed simulations.

In the non-standard neutrino hypothesis the discovery of a shape distortion in the positron energy spectrum of the far detectors may be determinant in disentangling θ_{13} from θ_{new}.

VII. TESTING THE ANOMALY

A. At reactors

The presence of sterile neutrinos would leave its imprint on the signal at both the near and far detectors of forthcoming reactor neutrino experiments. Taking results from multi-detectors and allowing for the possibility of sterile mixing angles, one can probe both θ_{13} and the sterile mixing angle θ_{new} at Daya Bay, Double Chooz, and RENO [37]. Positron spectrum energy distortions should be deeply investigated at near detectors, as quoted in [39]. In any case, measurements of the expected over predicted event rates at the near detectors will allow the probing of the reactor antineutrino anomaly, providing high statistics and high precision measurements at a few hundreds meters from the antineutrino sources. The antineutrino anomaly would be best tested by performing blind analyses for all near detector data.

Further measurements at very short baselines below 100 meters would be useful to confirm the MeV electron antineutrino deficit. Currently no fundamental research program is underway to search for new oscillation physics at reactors. However there is a worldwide program at short baselines for the purpose of nuclear non-proliferation, using antineutrinos as new IAEA safeguards tools [40]. In this context the Nucifer experiment, located 7 meters away from the Osiris research reactor core in Saclay, will start its operation in 2011 [41]. Nucifer will thus have the possibility to test the anomaly. A rate-only analysis with a precision of a few percent may not be enough to provide a decisive improvement of the understanding of the anomaly. But a shape analysis may provide enough information, depending of the energy resolution.

We note here that the antineutrino non-proliferation program will not be affected by the antineutrino anomaly since relative antineutrino rates with respect to known thermal power could be used to calibrate the experiments.

B. MegaCurie radioactive sources

As mentioned above, radio chemical gallium experiments (Gallex and Sage) tested their experimental procedure by exposing their gallium target to MegaCurie neutrino sources using ^{51}Cr or ^{37}Ar [44]. The production and handling of such devices is thus well under control. Ref. [51] proposed to use a ^{51}Cr source inside two concentric Gallium tanks, whereas Ref. [52] proposed to use a ^{51}Cr or ^{90}Sr source next to the Borexino detector. In liquid scintillating detectors ^{51}Cr or ^{37}Ar ν_e's are detected through neutrino-electron elastic scattering while ^{90}Sr $\bar{\nu}_e$'s are detected through inverse beta decay. With the Δm^2_{new} values best fitting the sterile neutrino hypothesis, the deployment of a radioactive source at the center of an ultra-low background neutrino detector, such as Borexino, KamLAND, and SNO+, would allow both the testing of the ν_e deficit and the search for an oscillation pattern as function of the detector radius. These neutrino sources emit quasi-mono-energetic neutrino lines of sub-MeV energies leading to a clear oscillation pattern at the range of a meter. In addition a ^{37}Ar source emits only γ-rays through second order processes and is therefore easy to handle after its irradiation inside a breeder nuclear reactor. As an example if a source of 1 MCi were inserted in the middle of a large detector like SNO+, it would provide a few hundred thousand interactions in the detector, of which a few ten thousands would deposit more than 500 keV. A <15 cm accurate vertex reconstruction could allow to draw a simple and clear figure of the number of neutrino interactions as the function of the radius directly testing the sterile neutrino oscillation pattern for Δm^2_{new} <5 eV^2.

VIII. CONCLUSIONS AND OUTLOOK

The impact of the new spectra of reactor antineutrino is extensively studied in this article. The increase of the expected antineutrino rate by about 3.5% combined with revised values of the antineutrino cross section significantly decreased the normalized ratio of observed to expected event rates in all previous reactor experiments performed over the last 30 years at distances below 100 m [2–8, 10, 31]. The averaged ratio is 0.937±0.027, leading to the reactor antineutrino anomaly. This deficit could still be due to some unknown in the reactor physics, but we also analyze these revised results in terms of a suppression of the $\bar{\nu}_e$ rate at short distance as we can expect from a sterile neutrino, beyond the standard model, with a large $|\Delta m^2_{new}| \gg \Delta m^2_{31}$. We note that hints of such results were already present at the ILL neutrino experiment in 1981 [23]. We also considered that other neutrino experiments, MiniBooNE [46] and the Gallium neutrino sources experiments [44], observe ν_e deficits at a similar L/E. These anomalies were comprehensively studied in Ref. [43]. It is important to note that these anomalies exist and are comparable in both the neutrino and the antineutrino sectors. Furthermore it turns out that each experiment fitted separately leads to similar values of $\sin^2(2\theta_{new})$ and similar lower bounds for $|\Delta m^2_{new}|$, but without a strong significance. Hence, we combined in a global fit these results with our re-evaluation of the reactor experiment results, taking into account the existing correlations. This leads to a solution for a new neutrino oscillation, such that $|\Delta m^2_{new}|$ >1.5 eV^2 (95% C.L.) and $\sin^2(2\theta_{new}) = 0.17 \pm 0.08$ (95% C.L.), disfavoring the no-oscillation case at 99.93% C.L. This hypothesis should be checked against systematical effects, either in the prediction of the reactor antineutrino spectra or in the experimental results.

We then revised the constraints on the θ_{13} mixing angle obtained with the three active neutrino oscillation framework by CHOOZ [10] and KamLAND [14]. We show that a $\bar{\nu}_e$ deficit measured at any antineutrino experiment with a baseline greater than 1 km could be misinterpreted as a hint for a non-zero value of θ_{13}. Accounting for a possible $|\Delta m^2_{new}|$-driven sterile neutrino oscillation we revise the constraint on the third mixing angle, such that $\sin^2(2\theta_{13}) < 0.095$. Note that the KamLAND best fit of the solar neutrino parameters are unchanged. However, the combination of KamLAND and CHOOZ leads to a best fit value of $\sin^2(2\theta_{13}) = -0.02^{+0.07}_{-0.07}$, in good agreement with the best fit value extracted from the combined analysis of solar neutrino data. This relaxes the tension between reactor and solar data, reviewed in Ref. [15].

If the existence of a fourth neutrino turns out to be verified we note that an 8% reduction of the total flux of solar neutrino must be taken into account when confronting with the experimental results. In particular the total neutrino ν flux measured by SNO [55], at 5.14±0.21 10^6 cm^{-2}.s^{-1}, is now in better agreement with the prediction of the (reduced) high-Z Sun Standard Model model, at 5.24±0.9 10^6 cm^{-2}.s^{-1}), and disfavors the (reduced) low-Z one (4.09±0.9 10^6 cm^{-2}.s^{-1}). We note that the high-Z model is also in good agreement with the data from helioseismology, contrarily to the low-Z model [56].

Assuming a hypothetical new neutrino ν_{new} heavier than the three active neutrinos we can briefly quantify its contribution to the effective masses searched for in β-decay and neutrino-less $\beta\beta$-decay experiments, as performed in Ref. [43]. The Tritium β-decay experiments have reported $m_\beta \lesssim 2$ eV (95%) [54]. A fourth neutrino with a mass in the eV range should contribute more than the active neutrinos, which are expected to have sub-eV masses, to the signal searched for in direct detection beta decay experiments. We find that the contribution of the fourth neutrino state fitting the data analyzed in this article would contribute to m_β for more than 0.2 eV (95% C.L.). This is within the sensitivity range of the forthcoming KATRIN experiment [57]. Assuming Majorana neutrinos, the contribution of the fourth state would be such that $m_{\beta\beta} \gtrsim 0.02$ eV (95% C.L.), which is above the contribution of the three active neutrinos and thus disfavors possible cancellations with the three other active flavors [43, 58]. This contribution is of interest for the

forthcoming experiments [59].

Furthermore we would like to stress that the existence of a fourth neutrino is slightly favored by some recent cosmological data. The effective number of neutrino species fitted by WMAP and BAO observations [60] is N_{eff}=4.34±0.87. An analysis of WMAP combined with the Atacama Cosmology Telescope data [61] leads to N_{eff}=5.3±1.3, and an independent analysis of the WMAP 7 years data [62] provides N_{eff}=4±1. Finally a recent analysis based on non-standard big bang nucleosynthesis [63] leads to N_{eff}=3.78±0.75. But the compatibility of the sterile neutrino hypothesis exposed in this paper ($|\Delta m^2_{new}| > 1.5$ eV^2, $\sin^2(2\theta_{new}) = 0.17$) with cosmological models and data should be assessed, especially its contribution to the non-baryonic dark matter of the Universe which may be non negligible.

Finally, a clear experimental proof of the presence of this fourth non-standard neutrino becomes mandatory. This can be given by the imprint on the energy spectrum in a very short baseline reactor neutrino experiment or by a new neutrino source experiment in a detector with energy and spatial resolution.

IX. ACKNOWLEDGMENTS

We would like to thank M. Fallot, J. Gaffiot, L. Giot, J. Martino, A. Porta, V. Rulhmann-Kleider, J.-L. Sida, and F. Yermia for their careful reading of this manuscript. We are grateful to H. de Kerret, J. Rich, and S. Schoenert for discussions and suggestions.

Appendix A: Error propagation in reactor experiment analyses

One of the main difficulties in these calculations is the propagation of the errors on the ILL data from [18–20] to the final result, i.e. the cross-section per fission for each of the isotopes. From our previous work in [16] we propagated the error on the ILL data and the conversion procedure to the resulting neutrino spectra. However the binning and the energy range are then those of the ILL data (250 keV bins from 2 to 8 MeV for ^{235}U).

These data are then fitted to an exponential-polynomial model, see for example [34]. This allows to use arbitrarily fine binning, which is necessary for the correct convolution with the inverse beta cross-section and also the oscillation probability. In [34] the authors outline a method to propagate the errors and correlations on the polynomial coefficients to the physical observable. However as they point out the correlation matrices obtained from the fit are rather unstable, most coefficients being strongly correlated or anti-correlated to each other. We found that this made error propagation very difficult.

As an exercise, we performed the following simple Monte-Carlo simulation: using the original correlation matrix on the converted ILL spectra, we simulated a series of ILL converted spectra, and fitted each of them using the exponential-polynomial model from [34]. We then evaluated the fitted polynomials in each energy bin, yielding fitted Monte-Carlo neutrino spectra. We then computed the bin-to-bin correlation matrix of these Monte-Carlo spectra.

An example of the result is shown in Figure 12, along with the original correlation matrix in Figure 11. Clearly the polynomial fit induces long-range correlations and anti-correlations between spectrum bins, and washes out the original correlations. We concluded that while we could rely on the polynomial fit for the mean values of the spectra (since the fit residuals are acceptably small), we could not use the resulting correlation matrices for error propagation.

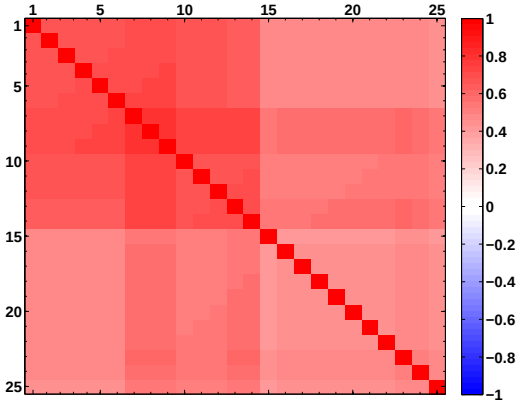

FIG. 11. Bin-to-bin correlation matrix (25x25 bins, 2-8 MeV) of converted neutrino spectrum from ^{235}U, including the ILL experimental errors and conversion effects from [16].

We therefore choose to propagate the original correlation matrix on our final binning by interpolating linearly between each bin of the original covariance matrix, and then computing the resulting correlation matrix. For bins which were not present in the original energy range, we take a constant error of 20%, fully correlated bin-to-bin in order to obtain a conservative upper bound on the error. This allows us to use any binning over any energy range. Of course the resulting matrix still has rank 25 over the 2-8 MeV range, but since we do not need its inverse this does not limit our ability to use it for error propagation. An example of the resulting matrix can be found in Figure 13 for ^{235}U.

Finally, as a cross-check of this method, we computed the error on the cross-section per fission for each isotope, using our new error propagation method with interpolated ILL and conversion correlation matrices (column 2 of table I, reproduced in table V below), and directly folding the converted ILL spectra with the inverse beta decay cross-section. Clearly, the results are extremely close. The effect of the error on the extrapolated part of

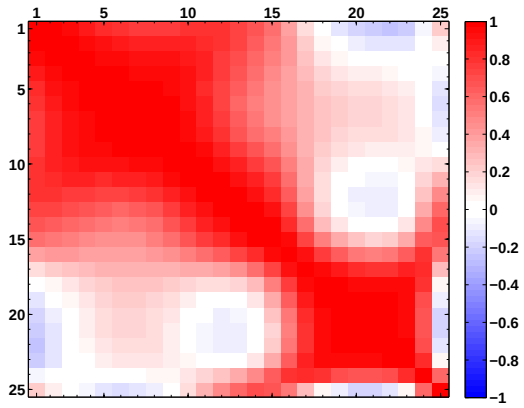

FIG. 12. Bin-to-bin correlation matrix (25x25 bins, 2-8 MeV) of fitted neutrino spectrum from ^{235}U, following the toy Monte-Carlo procedure outlined in the text. While the structure of Figure 11 is still present it has been significantly washed out and anti-correlation areas have appeared.

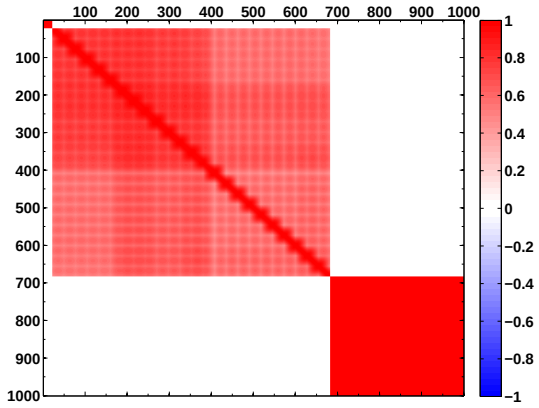

FIG. 13. Bin-to-bin correlation matrix (1000x1000 bins, 1.75-10 MeV) of the fitted neutrino spectrum from ^{235}U, obtained after linear interpolation of the original matrix, and extrapolating to a fully correlated 20% error outside the original binning. Clearly the experimental correlations from the ILL measurements are kept with this technique.

the spectrum is found to be negligible. We also verified that the resulting error bars do not significantly depend on the chosen binning. These calculations validate the use of the exponential-polynomial fit along with the interpolation technique for error propagation on the final spectrum, and allow us to use the binning of our choice without affecting the errors.

For ^{238}U, since the spectrum is obtained from *ab initio* calculations, each bin is given an error ranging from 10% at low energy to 20% at high energy. However, if these errors are uncorrelated, the uncertainty on the overall neutrino rate and hence the cross-section per fission for ^{238}U is artificially low. To avoid this, we consider that there is a fully correlated 10% error on bins from 2 to 5.5 MeV, another fully correlated 15% error on the block from 5.5 to 6.75 MeV and another 20% fully correlated error on the last bins of the spectrum. With this conservative prescription our error on the ^{238}U cross-section per fission is 8.2%.

Isotope	This work 1000 bins, 1.8-10 MeV	ILL spectra 25 bins, 2-8 MeV
σ_{U235}	6.61±2.11%	6.61±2.13%
σ_{Pu239}	4.34±2.45%	4.33±2.46%
σ_{Pu241}	5.97±2.15%	6.02±2.16%

TABLE V. Comparison between cross-sections per fission obtained from fitted spectra (central column), and from a direct convolution of the converted ILL spectra (right column). The error bars are 'exact' in the case of the direct convolution, while they are approximate for the fitted spectrum, obtained from interpolation of the original matrices.

Finally we derive the total error, $\sigma_{S_{tot}}$, on the antineutrino rate, for a given core composition. We account for the uncertainties on the cross section per fission per isotope, and the uncertainties on the averaged fraction of fission per isotopes. As an example we can consider the case of Bugey-4. The fuel composition is given in Ref. [3]. The new values of the cross sections per fission per isotope as well as their uncertainties are given in Table I. The f_k coefficients are taken as correlated, following a typical fuel evolution curve, and such that $\sum_k f_k$=1±0.6% to account for the error on the thermal power of the nuclear core. In a first case we consider a 10% relative uncertainty on the fuel composition of 10%. We obtain a final error on the expected number of events of 2.7%. Reducing the error on the fuel composition to 3.5% results in a final error of 2.4%.

Appendix B: Gallex/Sage, and MiniBooNE reanalysis

In this appendix we briefly provide details on our reanalysis of published data from Gallex ^{51}Cr source data [49, 50], SAGE ^{51}Cr [47] and ^{37}Ar source data [48], and MiniBooNE neutrino data [46].

The Gallex collaboration performed two measurements with two ^{51}Cr sources in [49], obtaining the ratio of the measured and expected event rates. These data were recently reanalyzed [50], providing updated values of the errors and the ratios. The SAGE collaboration performed a similar measurement with a ^{51}Cr source, and more recently with a ^{37}Ar source [47, 48]. An analysis of these data in terms of neutrino oscillation was performed in [43, 45]. The data values are 0.95 ± 0.11, 0.81 ± 0.11, 0.95 ± 0.12 and 0.79 ± 0.09. Performing a neutrino oscillation search with these values yields contours very close to

those of [43]. However we decided to include possible correlations between these four measurements in this present work, that were not previously taken into account. As the two Gallex measurements used the same experimental technique, we decided to fully correlate their systematic errors, which we understand to be 5.6% and 7.4% respectively. The statistical errors remain of course uncorrelated. For SAGE we followed a similar procedure, with systematics of 5.7% and 7.0% according to [47, 48].

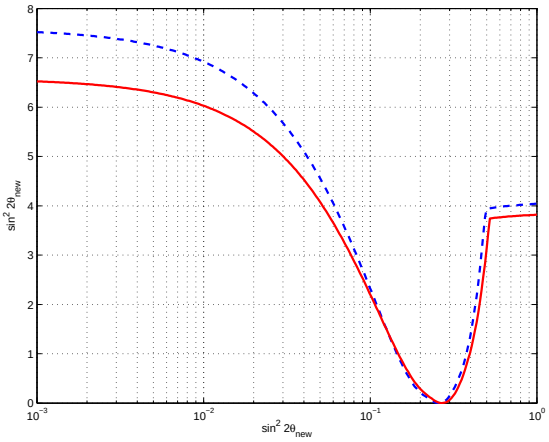

FIG. 14. Reanalysis of the gallium calibration data of Gallex and Sage. $\Delta\chi^2$ projections as a function of $\sin^2 2\theta$, without correlations (dashed) and with correlations as explained in the text. The dashed contour is very close to that of [43], validating this approach.

Our fractional covariance matrix is

$$\begin{pmatrix} 1.31 & 0.41 & 0 & 0 \\ 0.41 & 1.55 & 0 & 0 \\ 0 & 0 & 1.53 & 0.40 \\ 0 & 0 & 0.40 & 1.30 \end{pmatrix} 10^{-2}. \qquad \text{(B1)}$$

As expected we obtained slightly more conservative contours than those of [43] with this method.

We also analyzed the MiniBooNE neutrino data from [46] following the method outlined in [43]. The idea is to fit both electron-like and muon-like data at the same time. However, instead of searching for $\nu_\mu \to \nu_e$ appearance, we search for ν_e disappearance, while allowing the global normalization of all the samples (e-like and mu-like) to fluctuate. The excess of e-like data in the low energy part of the spectrum is well-fitted by the combined increase in overall normalization and by the disappearance of ν_e induced e-like events. We used a simplified version of the analysis in reference [43], in that we used a covariance matrix independent from the normalization fitting parameter f. We obtain very similar results, although our best fit point is in a slightly different location, at $\sin^2 2\theta = 0.23$, $\Delta m^2 = 1.88$ eV^2 and $f = 1.083$, as can be seen in Figure 15.

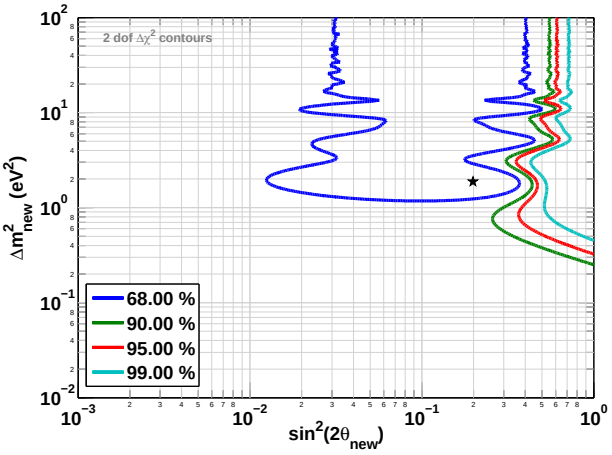

FIG. 15. Analysis of the MiniBOONE data following a procedure very similar to that of [43]. Our results are in good agreement.

We have only included this analysis of MiniBooNE's data for completeness. However in our final statistical significance it has very little impact.

[1] K. Nakamura *et al.*, (Particle Data Group), J. Phys. G **37**, 075021 (2010).
[2] H. Kwon *et al.*, Phys. Rev. D**24** 1097 (1981).
[3] Y. Déclais *et al.*, Phys. Lett. B**338** (1994) 383.
[4] B. Achkar *et al.*, Nucl. Phys. B**434** (1995) 503.
[5] G. Zacek *et al.*, Phys. Rev. D**34** (1986) 2621.
[6] V. Kuvshinnikov *et al.*, JETP **54** N5 (1991) 259.
[7] G.S. Vidyakin *et al.*, JETP. **93** (1987) 424-431.
[8] G.S. Vidyakin *et al.*, JETP Lett. **59** (1994) 390.
[9] Th. Lasserre and H.W. Sobel., Comptes Rendus Physique, French Academy of Sciences, **6**, 749-757 (2005) arXiv:nucl-ex/0601013.
[10] M. Apollonio *et al.*, Phys. Lett. **B466**, 415 (1999). M. Apollonio *et al.*, Eur. Phys. J. **C27**, 331-374 (2003).
[11] X. Guo *et al.*, arXiv:hep-ex/0701029.
[12] F. Ardellier *et al.*, arXiv:hep-ex/0606025.
[13] J. K. Ahn *et al.*, arXiv:hep-ex/1003.1391.
[14] A. Gando *et al.*, arXiv:1009.4771v2.
[15] M. Mezzetto, T. Schwetz, J. Phys. G**37**, 103001 (2010).
[16] Th. A. Mueller, D. Lhuillier *et al.*, arXiv:1101.2663 (submitted to PRC); Th. A. Mueller, PhD Thesis, Paris-Sud XI University, 2010.
[17] K. Schreckenbach *et al.*, Phys. Lett. **99B**, 251 (1981).
[18] K. Schreckenbach *et al.*, Phys. Lett. **160B**, 325 (1985).
[19] F. von Feilitzsch, A. A. Hahn and K. Schreckenbach, Phys. Lett. **118B**, 162 (1982).
[20] A. A. Hahn *et al.*, Phys. Lett. **218B**, 365 (1989).
[21] B. R. Davis *et al.*, Phys. Rev. C**19**, 2259 (1979). P. Vogel

et al., Phys. Rev. C**24**, 1543 (1981).
[22] N. H. Haag, Bestimmung des Antineutrinospektrums der Spaltprodukte von ^{238}U, Diplomarbeit, Technische Universität München.
[23] A. Hoummada *et al.*, Appl. Rad. Isot. Vol. 46, No. 6/7, pp. 449-450, (1995).
[24] D. Nicolo, Search for neutrino oscillations in a long baseline, experiment at the Chooz nuclear reactors, PhD (1999)
[25] P. Adamson *et al.*, Phys. Rev. Lett. **101**, 131802 (2008)
[26] P. Vogel, Phys. Rev. **D29**, 1918 (1984).
[27] P. Vogel *et al.*, Phys. Rev. C**24**, 1543 (1981).
[28] V.I. Kopeikin, Preprint Kurchatov Institut of Atomic energy, Moscow **IAE-4305/2**, (1988).
[29] L.A. Mikaelyan, JETP *Lett.* **47**, (1988).
[30] A.A. Kuvshinnikov *et al.*, *Sov. J. Nucl. Phys.* **52**, (1990) 300, JETP *Lett.* **54**, (1991) 255.
[31] F. Boehm Phys. Rev. **D64**, 11 (2001).
[32] K. Schreckenbach *et al.*, to be completed.
[33] http://www.iaea.org/programmes/a2/.
[34] P. Huber and T. Schwetz, Phys. Rev. D**70** (2004) 053011.
[35] G. Mention, T. Lasserre, and D. Motta, arXiv:0704.0498.
[36] J. J. Gomez-Cadenas and M. C. Gonzalez-Garcia, Z. Phys. **C71**, 443 (1996); S. Goswami, Phys. Rev. **D55**, 2931 (1997); S. M. Bilenky, C. Giunti and W. Grimus, Eur. Phys. J. C **1**, 247 (1998).
[37] A. Bandyopadhyay, S. Choubey arXiv:0707.2481v1.
[38] . M. Fallot *et al.*, to be published.
[39] A. de Gouvea and T. Wytock arXiv:0809.5076.
[40] IAEA Final Report: Focused Workshop on Antineutrino Detection for Safeguards Applications (2008)
[41] A. Porta *et al.*, J. Phys. Conf. Ser. **203** 012092 (2010).
[42] C. Giunti, M. Laveder, Phys. Rev. D**80** (2009) 013005.
[43] C. Giunti, M. Laveder, Phys. Rev. D**82** (2010) 053005.
[44] P. Anselmann *et al.* (GALLEX), Phys. Lett. B**342**, 440 (1995); W. Hampel *et al.* (GALLEX), Phys. Lett. B**420**, 114 (1998); F. Kaether *et al.* Phys. Lett. B**685**, 47 (2010); J. N. Abdurashitov *et al.* (SAGE), Phys. Rev. Lett. **77**, 4708 (1996); J. N. Abdurashitov *et al.* (SAGE), Phys. Rev. C**59**, 2246 (1999); J. N. Abdurashitov *et al.*, Phys. Rev. C**73**, 045805 (2006); J. N. Abdurashitov *et al.* (SAGE), Phys. Rev. C**80**, 015807 (2009).
[45] C. Giunti, M. Laveder, arXiv:1006.3244v2.
[46] A. A. Aguilar-Arevalo *et al.*, Phys. Rev. Lett. **98** (2007) 231801.; A. A. Aguilar-Arevalo *et al.*, Phys. Rev. Lett. **102** (2009) 101802.
Data release available at www-boone.fnal.gov/
[47] J. N. Abdurashitov *et al.*, Phys. Rev. C **59**, 2246 (1999). arXiv:hep-ph/9803418.
[48] J. N. Abdurashitov *et al.*, Phys. Rev. C **73**, 045805 (2006)
[49] W. Hampel *et al.*, Phys. Lett. B **420**, 114 (1998).
[50] F. Kaether, W. Hampel *et al.*, Phys. Lett. B **685** (2010) 47-54.
[51] V. N. Gavrin, V. V. Gorbachev, E. P. Veretenkin, B. T. Cleveland arXiv:1006.2103.
[52] A. Ianni , D. Montanino, G. Scioscia, Eur. Phys. J. C8 (1999) 609-617.
[53] F. Reines, H. W. Sobel, F. Pasierb, Phys. Rev. Lett. **45** (1980) 1307-1311. F. James, Lecture at the CERN School of Computing, CERN DD/81/02, 1980.
[54] C. Kraus *et al.*, Eur. Phys. J. C40, 447 (2005); V. M. Lobashev, Nucl. Phys. A719, C153 (2003).
[55] B. Aharmim *et al.*, The SNO Collaboration, Phys. Rev. C **81**, 055504 (2010)
[56] C. PenaGaray, and A. Serenelli arXiv:0811.2424.
[57] KATRIN Collaboration, arXiv:hep-ex/0109033v1.
[58] M. Maltoni, T. Schwetz, M. A. Tortola, J. W. F. Valle, New J. Phys. 6:122,2004.
[59] M. Pedretti *et al.*, International Journal of Modern Physics A, 23 (2008) 3395; H. Simgen *et al.*, Nucl. Phys. B143 (2005) 567; R. Arnold *et al.*, Eur. Phys. J. CDOI 10.1140/epjc/s10052-010-1481-5 (2010).
[60] E. Komatsu *et al.*, arxiv.org/abs/1001.4538.
[61] J. Dunkley *et al.*, arxiv.org/abs/1009.0866.
[62] J. Hamann, S. Hannestad, G. G. Raffelt, I. Tamborra, and Y. Y.Y. Wong, arxiv.org/abs/1006.5276.
[63] Y. I. Izotov, T. X. Thuan, arxiv.org/abs/1001.4440.